On the comparison of asymptotic expansion techniques for the nonlinear Klein–Gordon equation in the nonrelativistic limit regime

Katharina Schratz, Xiaofei Zhao

KARLSRUHE INSTITUTE OF TECHNOLOGY

CRC 1173

Participating universities

Universität Stuttgart

EBERHARD KARLS
UNIVERSITÄT
TÜBINGEN

Funded by

DFG

ON THE COMPARISON OF ASYMPTOTIC EXPANSION TECHNIQUES FOR THE NONLINEAR KLEIN-GORDON EQUATION IN THE NONRELATIVISTIC LIMIT REGIME

KATHARINA SCHRATZ AND XIAOFEI ZHAO

ABSTRACT. This work concerns the time averaging techniques for the nonlinear Klein-Gordon (KG) equation in the nonrelativistic limit regime which have recently gained a lot attention in numerical analysis. This is due to the fact that the solution becomes highly-oscillatory in time in this regime which causes the breakdown of classical integration schemes. To overcome this numerical burden various novel numerical methods with excellent efficiency were derived in recent years. The construction of each method thereby requests essentially the averaged model of the problem. However, the averaged model of each approach is found by different kinds of asymptotic approximation techniques reaching from the modulated Fourier expansion over the multiscale expansion by frequency up to the Chapman-Enskog expansion. In this work we give a first comparison of these recently introduced asymptotic series, reviewing their approximation validity to the KG in the asymptotic limit, their smoothness assumptions as well as their geometric properties, e.g., energy conservation and long-time behaviour of the remainder.

1. INTRODUCTION

In this paper, we consider the dimensionless nonlinear Klein-Gordon (KG) equation in d-dimensions ($d = 1, 2, 3$) [5, 4, 16, 17, 19, 7]:

$$\begin{cases} \varepsilon^2 \partial_{tt} u(\mathbf{x}, t) - \Delta u(\mathbf{x}, t) + \dfrac{1}{\varepsilon^2} u(\mathbf{x}, t) + f(u(\mathbf{x}, t)) = 0, \quad \mathbf{x} \in \mathbb{R}^d, \quad t > 0, \\ u(\mathbf{x}, 0) = \phi_1(\mathbf{x}), \quad \partial_t u(\mathbf{x}, 0) = \dfrac{1}{\varepsilon^2} \phi_2(\mathbf{x}), \quad \mathbf{x} \in \mathbb{R}^d. \end{cases} \quad (1.1)$$

Here t is the time, $\mathbf{x}$ is the spatial variable, $u = u(\mathbf{x}, t)$ is a unknown real-valued scalar field and $0 < \varepsilon \leq 1$ is a dimensionless parameter inversely proportional to the speed of light. ϕ_1 and ϕ_2 are given real-valued initial data independent of ε and $f : \mathbb{R} \to \mathbb{R}$ is a given nonlinear function. It is a model widely occurred in quantum and particle physics.

The so-called non relativistic limit $\varepsilon \to 0$ of the KG equation (1.1) has been extensively studied in literature from a physical and mathematical point of view. Nowadays it is well understood that the KG equation converges to a nonlinear Schrödinger (NLS) equation when ε tends to zero. In Section 2 below we present the detailed structure of the NLS limit system. For recent analytic approximations results we refer to [26, 24, 25], and in the context of Birkhoff normal form transformations in particular to the recent work [28], as well as the references therein.

From a numerical point of view, however, the Klein-Gordon equation in the non-relativistic was an open problem for a long time. Classical methods are not able to resolve the highly-oscillatory nature of the solution which leads to severe step size restrictions (at least at order $\tau = \mathcal{O}(\varepsilon^{-2})$) and huge computational costs ([5]). This failure of classical integration schemes triggered intensive studies on the numerical averaging of the model, serving to describe better asymptotic behaviour of the solution and to design efficient numerical approximations. Based on this idea, very recently novel numerical integrators were proposed which allow us to numerically solve the KG equation (1.1) in the non relativistic regime $\varepsilon \to 0$, capturing the highly-oscillatory behaviour of the solution.

Three novel schemes for the Klein-Gordon equation in the non relativistic limit regime were presented so far in literature [19, 4, 12]. Each of the proposed numerical schemes for KG is essentially based on an *asymptotic expansion techinque* for the averaged model, and each of the asymptotic expansion is mathematically obtained by *different analytic techniques*, reaching from the modulated Fourier expansion (see, e.g., [21, 15, 18, 19]) over multiscale expansion by frequency (see, e.g., [4, 6, 8, 9]) up to the Chapman-Enskog expansion (see, e.g., [12, 14]).

The aim of this work is to for the first time give a comparison of the novel techniques, highlighting the gap to the KG in the asymptotic limit, reviewing their approximation validity, their geometric properties (e.g., energy conservation), the regularity requirement of each expansion to maintain the optimal asymptotic order, and the long-time behaviour of the expansion. It is worth noting that the asymptotic series [28] found by the Birkhoff normal form transformation is the same as the one derived from the modulated Fourier expansion [19]. In our analysis, we in particular focus on the three asymptotic methods: the modulated Fourier expansion [19], the multiscale expansion by frequency [4] and the Chapman-Enskog expansion [12]. Each expansion allows at leading order a remainder at order $\mathcal{O}(\varepsilon^2)$ in the approximation of the KG solution (1.1). However, each expansion is based on different mathematically techniques, allowing *different approximation validity*. This will be highlighted in Section 2.4 on the dynamics and comparison of the expansions, and underlined with numerical experiments.

We will consider in the following as most of the work in the literature did [4, 7, 5], the cubic nonlinearity case, i.e.

$$f(u(\mathbf{x}, t)) = \lambda u(\mathbf{x}, t)^3, \tag{1.2}$$

for some given constant $\lambda \in \mathbb{R}$. More importantly, under this case, the concerned asymptotic expansions of the solution of KG as $\varepsilon \to 0$ could be derived in explicit forms. When $\lambda < 0$, the solution of KG has finite time blow-up [1]. Hence, our discussion is always away from the maximum existence time of solution $T^* > 0$.

The paper is organized as follows. In Section 2, we present and compare the leading order version of the modulated Fourier expansion, the multiscale expansion by frequency and the Chapman-Enskog expansion. The higher order version the three expansions and results are presented in Section 3. Conclusions are drawn in Section 4.

2. Leading order expansion

In this section, we revise the modulated Fourier expansion [19], the multiscale frequency expansion [4] and the Chapman-Enskog expansion [12] of the KG (1.1) up to the leading order terms.

2.1. Modulated Fourier expansion.

The modulated Fourier expansion is a well known approach in the mathematical and numerical analysis of oscillatory problems (e.g., [15, 18, 21]). This technique was also recently introduced ([19]) as a numerical integrator for the KG equation (1.1) in the non relativistic regime $\varepsilon \to 0$. The general idea lies in expanding the solution according to the frequency and amplitude of the small parameter, i.e. for the KG (1.1)

$$u(\mathbf{x}, t) = \sum_{m \in \mathbb{N}_+} e^{imt/\varepsilon^2} u_m(\mathbf{x}, t),$$

where the functions $u_m(\mathbf{x}, t)$ have all the time derivatives uniformly bounded as $\varepsilon \to 0$ (for sufficiently smooth solutions). Up to the leading order term, i.e. $m = 1$, the modulated Fourier expansion of the solution of the KG (1.1), reads [25, 19]

$$u(\mathbf{x}, t) = e^{it/\varepsilon^2} z(\mathbf{x}, t) + e^{-it/\varepsilon^2} \overline{z}(\mathbf{x}, t) + o(1), \quad \varepsilon \to 0, \tag{2.1}$$

where $z(\mathbf{x}, t)$ solves the smooth (not highly oscillatory) nonlinear Schrödinger equation

$$\begin{cases} 2i\partial_t z(\mathbf{x}, t) - \Delta z(\mathbf{x}, t) + 3\lambda |z(\mathbf{x}, t)|^2 z(\mathbf{x}, t) = 0, & \mathbf{x} \in \mathbb{R}^d, \quad t > 0, \\ z(\mathbf{x}, 0) = \dfrac{1}{2} \left[\phi_1(\mathbf{x}) - i\phi_2(\mathbf{x}) \right], & \mathbf{x} \in \mathbb{R}^d. \end{cases} \tag{2.2}$$

The convergence from $u(\mathbf{x}, t)$ to $u_{MFo}(\mathbf{x}, t)$

$$u_{MFo}(\mathbf{x}, t) = e^{it/\varepsilon^2} z(\mathbf{x}, t) + e^{-it/\varepsilon^2} \overline{z}(\mathbf{x}, t) \tag{2.3}$$

as $\varepsilon \to 0$ – up to the maximum existence time of the solution – has been rigorously proven in some energy space, see for instance the recent work [24, 25]. Here, we give a short time justification with address of the convergence rate in terms of ε and the required regularity.

Lemma 2.1. *Define $R(\mathbf{x}, t) = u(\mathbf{x}, t) - u_{MFo}(\mathbf{x}, t)$. Under the assumption that $\phi_1, \phi_2 \in H^{m_0+4}(\mathbb{R}^d)$, $m_0 > d/2$, we have*

$$\|R(\cdot, t)\|_{H^{m_0}} \lesssim \varepsilon^2, \quad 0 \leq t \leq T, \tag{2.4}$$

for some T independent of ε and $0 < T < T^*$.

Remark 2.2. Here we give a new (shorter) proof of the general result obtained in [19] for the leading order ε^2. Our regularity assumptions on the solution nevertheless go in line with [19, Theorem 2] (with $\varepsilon = c^{-1}$).

Proof of Lemma 2.1. Plugging $u = u_{MFo} + R$ into the KG equation (1.1), we get

$$e^{it/\varepsilon^2} \left[\varepsilon^2 \partial_{tt} z + 2i\partial_t z - \Delta z \right] + e^{-it/\varepsilon^2} \left[\varepsilon^2 \partial_{tt} \overline{z} - 2i\partial_t \overline{z} - \Delta \overline{z} \right]$$

$$+ \varepsilon^2 \partial_{tt} R + \Delta R + \frac{R}{\varepsilon^2} + f(u) = 0.$$

The cubic nonlinearity $f(u)$ can be expanded as

$$f(u) = e^{it/\varepsilon^2} 3\lambda |z|^2 z + e^{-it/\varepsilon^2} 3\lambda |z|^2 \overline{z} + e^{3it/\varepsilon^2} \lambda z^3 + e^{-3it/\varepsilon^2} \lambda \overline{z}^3 + f_R,$$

with

$$f_R := 6\lambda|z|^2 R + \mathrm{e}^{2it/\varepsilon^2} 3\lambda z^2 R + \mathrm{e}^{-2it/\varepsilon^2} 3\lambda\overline{z}^2 R + \mathrm{e}^{it/\varepsilon^2} 3\lambda z R^2 + \mathrm{e}^{-it/\varepsilon^2} 3\lambda\overline{z} R^2 + R^3.$$

Since z satisfies the NLS equation (2.2), so we have

$$\varepsilon^2 \partial_{tt} R(\mathbf{x},t) + \Delta R(\mathbf{x},t) + \frac{R(\mathbf{x},t)}{\varepsilon^2} + \mathrm{e}^{3it/\varepsilon^2}\lambda z(\mathbf{x},t)^3 + \mathrm{e}^{-3it/\varepsilon^2}\lambda\overline{z}(\mathbf{x},t)^3 \qquad (2.5)$$
$$+ \mathrm{e}^{it/\varepsilon^2}\varepsilon^2 \partial_{tt} z(\mathbf{x},t) + \mathrm{e}^{-it/\varepsilon^2}\varepsilon^2 \partial_{tt}\overline{z}(\mathbf{x},t) + f_R(\mathbf{x},t) = 0, \quad \mathbf{x} \in \mathbb{R}^d, \ t > 0.$$

At $t = 0$, according to the expansion we have

$$z(\mathbf{x},0) + \overline{z}(\mathbf{x},0) + R(\mathbf{x},0) = \phi_1(\mathbf{x}), \quad \mathbf{x} \in \mathbb{R}^d,$$

$$\frac{i}{\varepsilon^2}\left[z(\mathbf{x},0) - \overline{z}(\mathbf{x},0)\right] + \partial_t z(\mathbf{x},0) + \partial_t\overline{z}(\mathbf{x},0) + \partial_t R(\mathbf{x},0) = \frac{\phi_2(\mathbf{x})}{\varepsilon^2}.$$

Hence by noting in (2.2) $z(\mathbf{x},0) = \frac{1}{2}(\phi_1(\mathbf{x}) - i\phi_2(\mathbf{x}))$, we get

$$R(\mathbf{x},0) = 0, \quad \partial_t R(\mathbf{x},0) = -\partial_t z(\mathbf{x},0) - \partial_t\overline{z}(\mathbf{x},0),$$

and from the NLS equation, we can further get

$$\partial_t R(\mathbf{x},0) = Im\left(-\Delta z(\mathbf{x},0) + 3\lambda|z(\mathbf{x},0)|^2 z(\mathbf{x},0)\right) \in H^{m_0+2}(\mathbb{R}^d).$$

Using Duhamel's principle in the Fourier space of (2.5), we have

$$\hat{R}(\xi,t) = \frac{\sin(\omega_\xi t)}{\omega_\xi}\hat{R}'(\xi,0) - \int_0^t \frac{\lambda\sin(\omega_\xi(t-\theta))}{\varepsilon^2\omega_\xi}\hat{F}_R(\xi,\theta)d\theta, \qquad (2.6)$$
$$- \int_0^t \frac{\lambda\sin(\omega_\xi(t-\theta))}{\varepsilon^2\omega_\xi}\left[\mathrm{e}^{3i\theta/\varepsilon^2}\widehat{(z^3)}(\xi,\theta) + \mathrm{e}^{-3i\theta/\varepsilon^2}\widehat{(\overline{z}^3)}(\xi,\theta)\right]d\theta$$
$$- \int_0^t \frac{\sin(\omega_\xi(t-\theta))}{\omega_\xi}\left[\mathrm{e}^{i\theta/\varepsilon^2}\widehat{z}''(\xi,\theta) + \mathrm{e}^{-i\theta/\varepsilon^2}\widehat{\overline{z}}''(\xi,\theta)\right]d\theta,$$

for $\omega_\xi = \frac{1}{\varepsilon^2}\sqrt{1 + \varepsilon^2|\xi|^2}$. The second integral term does not have resonance in the oscillatory part for $|\xi| \lesssim 1/\varepsilon^2$, and we can use a integration-by-part to see

$$\int_0^t \frac{\sin(\omega_\xi(t-\theta))}{\varepsilon^2\omega_\xi}\mathrm{e}^{3i\theta/\varepsilon^2}d\theta = \frac{\varepsilon^2\omega_\xi(\mathrm{e}^{3it/\varepsilon^2} - \cos(\omega_\xi t)) - 3i\sin(\omega_\xi t)}{\omega_\xi(\varepsilon^4\omega_\xi^2 - 9)} = O(\varepsilon^2).$$

By differentiating the NLS, we see $\partial_{tt} z \in H^{m_0}$. Noting $F_R = O(R)$, we can use the bootstrap argument to show assertion (2.4). $\qquad \square$

In a natural way, the limit model should be completely independent of ε. The NLS equation (2.2) obtained by the modulated Fourier expansion is the classical limit model of KG widely used among physicists [29, 20]. In [25] it is shown that if the initial data of KG (1.1) is perturbed by an $O(\varepsilon)$ function, i.e.

$$u(\mathbf{x},0) = \phi_1(\mathbf{x}) + \varepsilon\varphi_1(\mathbf{x}), \quad \partial_t u(\mathbf{x},0) = \frac{\sqrt{1-\varepsilon^2\Delta}}{\varepsilon^2}\left(\phi_2(\mathbf{x}) + \varepsilon\varphi_2(\mathbf{x})\right),$$

for some φ_1, φ_2 independent of ε, then the remainder of the leading order modulated Fourier expansion is no longer $O(\varepsilon^2)$. Instead, one only obtains asymptotically that

$$u(\mathbf{x},t) = u_{MFo}(\mathbf{x},t) + O(\varepsilon), \quad \varepsilon \to 0.$$

To improve the asymptotic convergence and obtain a remainder of order $O(\varepsilon^2)$, one has to include the next term in modulated Fourier expansion. In detail, the improved expansion (up to second order) reads

$$u(\mathbf{x}, t) = e^{it/\varepsilon^2} \left[z(\mathbf{x}, t) + \varepsilon w(\mathbf{x}, t) \right] + e^{-it/\varepsilon^2} \left[\overline{z}(\mathbf{x}, t) + \varepsilon \overline{w}(\mathbf{x}, t) \right] + O(\varepsilon^2), \qquad (2.7)$$

where z solves the NLS (2.2) and w solves a Schrödinger-type coupled nonlinear equation (for details see also [25])

$$\begin{cases} 2i\partial_t w(\mathbf{x}, t) - \Delta w(\mathbf{x}, t) + 3\lambda \left[2|z(\mathbf{x}, t)|^2 w(\mathbf{x}, t) + z(\mathbf{x}, t)^2 \overline{w}(\mathbf{x}, t) \right] = 0, \ t > 0, \\ w(\mathbf{x}, 0) = \dfrac{1}{2} \left[\varphi_1(\mathbf{x}) - i\varphi_2(\mathbf{x}) \right], \quad \mathbf{x} \in \mathbb{R}^d. \end{cases} \qquad (2.8)$$

In the proof of Lemma 2.1 we can readily include a perturbation at order $O(\varepsilon)$. More precisely, let us take a $O(\varepsilon)$ correction in the initial data of the NLS model (2.2), i.e.,

$$z(\mathbf{x}, 0) = \frac{1}{2} \left(u(\mathbf{x}, 0) - i\varepsilon^2 \partial_t u(\mathbf{x}, 0) \right), \qquad (2.9)$$

then the proof of Lemma 2.1 is still valid and we readily obtain that

$$u(\mathbf{x}, t) = u_{MFo}(\mathbf{x}, t) + O(\varepsilon^2), \quad \varepsilon \to 0.$$

In particular, we do not need to include further equations from the higher order term in the modulated Fourier expansion. Getting the higher order approximation of the model with less involved equations, is certainly more efficient in the numerical simulation. Here the NLS (2.2) can be easily solved by splitting methods (see for instance [23]).

In the following, we will refer to the classical expansion (2.7) as the two-term expansion, and for the expansion (2.1) with high order corrections (2.9) as the one-term expansion. The aim is to study and compare the two approaches numerically. We choose the initial value in (1.1) as follows

$$u(\mathbf{x}, 0) = \frac{sech(x^2)}{2} + \varepsilon e^{-x^2}, \ \partial_t u(\mathbf{x}, 0) = \frac{\sqrt{1 - \varepsilon^2 \Delta}}{\varepsilon^2} \left[\frac{e^{-x^2}}{2} + \varepsilon \frac{sech(x^2)}{\sqrt{2}} \right],$$

and numerically simulate the remainder of the two kinds of expansions. The remainders in the H^1-norm at $T = 0.5$ and $T = 1$ under different ε are shown in Table 1. The dynamics of the remainders $\|R\|_{H^1}/\varepsilon^2$ are plotted in Figure 1. As can be seen from the results, the approximations of the two approaches are quite close. The H^1-norm of the remainders of the expansions are both linearly increasing with respect to time. Therefore, we conclude that the one-term expansion approach is more efficient numerically. The same strategy applies to all the other expansions presented below. Hence, we shall not address this issue any further.

2.2. **Multiscale frequency expansion.** The multiscale frequency expansion is introduced in [4, 6, 8, 9]. Formally, it goes similarly as the modulated Fourier expansion, i.e. $u(\mathbf{x}, t) = \sum_{m \in \mathbb{N}_+} e^{imt/\varepsilon^2} u_m(\mathbf{x}, t)$, but it allows ε-dependent perturbations and oscillations in the function u_m. The important thing is that $u_m(\mathbf{x}, t)$ oscillates much weaker than the original solution $u(\mathbf{x}, t)$ in time. In other words, the time derivatives of $u_m(\mathbf{x}, t)$ up to some order are uniformly bounded as $\varepsilon \to 0$. The leading order expansion for the KG (1.1) as given in [4] reads

$$u(\mathbf{x}, t) = e^{it/\varepsilon^2} z^\varepsilon(\mathbf{x}, t) + e^{-it/\varepsilon^2} \overline{z^\varepsilon}(\mathbf{x}, t) + o(1), \quad \varepsilon \to 0, \qquad (2.10)$$

TABLE 1. Remainders (in H^1-norm) of the classical two-term expansion and the one-term with perturbation

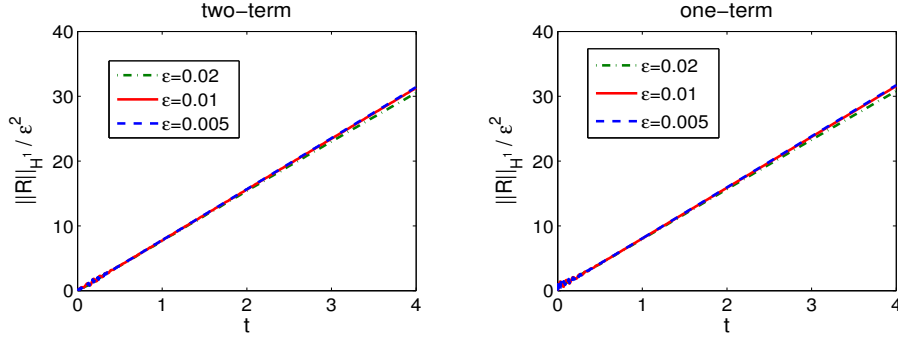| $t = 0.5$	$\varepsilon = 0.05$	$\varepsilon/2$	$\varepsilon/2^2$	$\varepsilon/2^3$
two-term	9.00E-3	2.40E-3	5.98E-4	1.51E-4
one-term	9.60E-3	2.50E-3	6.45E-4	1.64E-4
$t = 1$	$\varepsilon = 0.05$	$\varepsilon/2$	$\varepsilon/2^2$	$\varepsilon/2^3$
two-term	1.79E-2	4.80E-3	1.20E-3	3.05E-4
one-term	1.84E-2	4.90E-3	1.30E-3	3.15E-4

FIGURE 1. Behavior of the remainder $\|R\|_{H^1}/\varepsilon^2$ of the two-term expansion and the one-term expansion with respect to time.

where $z^\varepsilon(\mathbf{x}, t)$ solves the nonlinear Schrödinger equation with wave operator (NLSW)

$$\begin{cases} 2i\partial_t z^\varepsilon(\mathbf{x}, t) + \varepsilon^2 \partial_{tt} z^\varepsilon(\mathbf{x}, t) - \Delta z^\varepsilon(\mathbf{x}, t) + 3\lambda |z^\varepsilon(\mathbf{x}, t)|^2 z^\varepsilon(\mathbf{x}, t) = 0, \ \mathbf{x} \in \mathbb{R}^d, \ t > 0, \\ z^\varepsilon(\mathbf{x}, 0) = \frac{1}{2} \left[\phi_1(\mathbf{x}) - i\phi_2(\mathbf{x}) \right], \ \mathbf{x} \in \mathbb{R}^d, \\ \partial_t z^\varepsilon(\mathbf{x}, 0) = \frac{i}{2} \left[-\Delta z^\varepsilon(\mathbf{x}, 0) + 3\lambda |z^\varepsilon(\mathbf{x}, 0)|^2 z^\varepsilon(\mathbf{x}, 0) \right], \ \mathbf{x} \in \mathbb{R}^d. \end{cases} \quad (2.11)$$

The above NLSW with the so-called well-prepared initial data offers [4] $\partial_t^k z^\varepsilon(\mathbf{x}, t) = O(1)$ for $k = 0, 1, 2$, as $\varepsilon \to 0$, and the expansion

$$u_{MFe}(\mathbf{x}, t) = e^{it/\varepsilon^2} z^\varepsilon(\mathbf{x}, t) + e^{-it/\varepsilon^2} \overline{z}^\varepsilon(\mathbf{x}, t)$$

has the estimate [4]:

Lemma 2.3. *Define $R(\mathbf{x}, t) = u(\mathbf{x}, t) - u_{MFe}(\mathbf{x}, t)$. Under the assumption that $\phi_1, \phi_2 \in H^{m_0+2}(\mathbb{R}^d)$, $m_0 > d/2$, we have*

$$\|R(\cdot, t)\|_{H^{m_0}} \lesssim \varepsilon^2, \quad 0 \le t \le T, \quad (2.12)$$

for some T independent of ε and $0 < T < T^*$.

The proof can be carried out similarly to the proof of Lemma 2.1 and will be therefor omitted. For a detailed proof we refer to [4].

Comparison of Modulated Fourier Expansion and Multiscale Frequency Expansion: Comparing the approximation result in Lemma 2.3 to Lemma 2.1 we observe

that the multiscale frequency expansion (2.10) requires less regularity assumptions on the exact solution than the modulated Fourier expansion (2.1) to get optimal quadratic convergence in ε. This can be formally justified as follows: Note that in the multiscale frequency expansion the second order time derivative term $\partial_{tt} z^\varepsilon$ is the dominant term in the equation of z^ε, whereas the modulated Fourier expansion suffers from a less regular source term in the remainder's equation (see (2.5)). This leads to stronger regularity requirements on the solution in the latter.

The drawback of the mulsticale frequency expasion is that the limit model NLSW (2.11) is still highly oscillatory. One can solve (2.11) by exponential integrators [3, 30, 22] with uniform accuracy up to second order for all $0 < \varepsilon \leq 1$, since $\partial_{tt} z = O(1)$. However, to obtain higher order numerical methods, one will again need to incorporate a CFL-type condition restricting the time step by ε.

2.3. **Chapman-Enskog expansion.** The Chapman-Enskog expansion is origi- nal used to derive the Navier-Stokes equation from the Boltzmann equation, and is nowadays a popular tool for analysis in thermal dynamics [11]. In [12], the Chapman-Enskog expansion has been applied to the nonlinear KG. Thereby, in a first step we have to transform the KG wave equation into a first-order system in time. This will allow a form, where the fast time scale contributes at the next order term of the asymptotic series.

This is achieved by introducing the new variable (see [12] for the detailed con- struction)

$$v(\mathbf{x},t) = u(\mathbf{x},t) - i\varepsilon^2(1-\varepsilon^2\Delta)^{-1/2}\partial_t u(\mathbf{x},t).$$

This transformation allows to write the KG (1.1) as a first order system in time

$$\begin{cases} i\partial_t v = -\dfrac{1}{\varepsilon^2}(1-\varepsilon^2\Delta)^{1/2}v - \dfrac{\lambda}{8}(1-\varepsilon^2\Delta)^{-1/2}\left(v+\overline{v}\right)^3, \\ v(\mathbf{x},0) = v_0(\mathbf{x}) := \phi_1(\mathbf{x}) - i(1-\varepsilon^2\Delta)^{-1/2}\phi_2(\mathbf{x}). \end{cases}$$

By introducing the filtered variable

$$w(\mathbf{x},t) = \mathrm{e}^{-it/\varepsilon^2\sqrt{1-\varepsilon^2\Delta}}v(\mathbf{x},t),$$

one furthermore obtains that

$$\begin{cases} \partial_t w = \dfrac{i\lambda}{8}(1-\varepsilon^2\Delta)^{-1/2}\mathrm{e}^{-it/\varepsilon^2\sqrt{1-\varepsilon^2\Delta}}\left(\mathrm{e}^{it/\varepsilon^2\sqrt{1-\varepsilon^2\Delta}}w + \mathrm{e}^{-it/\varepsilon^2\sqrt{1-\varepsilon^2\Delta}}\overline{w}\right)^3, \\ w(\mathbf{x},0) = v_0(\mathbf{x}). \end{cases} \tag{2.13}$$

We observe from the above equation that the new unknown function $w(\mathbf{x},t)$ satisfies

$$w(\mathbf{x},t) = O(1), \quad \partial_t w(\mathbf{x},t) = O(1), \quad \partial_{tt} w(\mathbf{x},t) = O(\varepsilon^{-2}), \quad \varepsilon \to 0,$$

which indicates that the fast time scale t/ε^2 does not appear in the leading order expansion of $w(\mathbf{x},t)$.

Next, we isolate the fast time scale t/ε^2 in (2.13). This will allow us to carry out a time averaging technique later on. Define

$$D_\varepsilon = \frac{1}{\varepsilon^2}\left[\sqrt{1-\varepsilon^2\Delta} - 1\right],$$

$$F(t,\xi,\phi) := \frac{i\lambda}{8}(1-\varepsilon^2\Delta)^{-1/2}\mathrm{e}^{-i\xi}\mathrm{e}^{-itD_\varepsilon}\left(\mathrm{e}^{i\xi}\mathrm{e}^{itD_\varepsilon}\phi + \mathrm{e}^{-i\xi}\mathrm{e}^{-itD_\varepsilon}\overline{\phi}\right)^3,$$

such that (2.13) reads

$$\partial_t w(\mathbf{x},t) = F(t,t/\varepsilon^2,w(\mathbf{x},t)), \quad \mathbf{x} \in \mathbb{R}^d, \ t > 0. \tag{2.14}$$

Here it is important to note the 2π-periodicity of $F(t, \xi, \phi)$ in the ξ variable. The Chapmam-Enskog expansion for w then reads as

$$w(\mathbf{x}, t) = \underline{w}(\mathbf{x}, t) + o(1), \quad \varepsilon \to 0,$$

where $\underline{w}(\mathbf{x}, t)$ solves the averaged equation

$$\partial_t \underline{w}(\mathbf{x}, t) = \Pi F(t, \xi, \underline{w}(\mathbf{x}, t)) := \frac{1}{2\pi} \int_0^{2\pi} F(t, \xi, \underline{w}(\mathbf{x}, t)) \, d\xi, \quad \mathbf{x} \in \mathbb{R}^d, \ t > 0,$$

with $\underline{w}(\mathbf{x}, 0) = w(\mathbf{x}, 0)$. Since we are considering the cubic nonlinearity, i.e. $f(u) = \lambda u^3$, the average of $F(t, \xi, \phi)$ in ξ can be written down explicitly, In particular, we obtain the following leading order equation (or limit model)

$$\begin{cases} \partial_t \underline{w}(\mathbf{x}, t) = \dfrac{3i\lambda}{8\sqrt{1 - \varepsilon^2 \Delta}} \mathrm{e}^{-itD_\varepsilon} \left| \mathrm{e}^{itD_\varepsilon} \underline{w} \right|^2 \left(\mathrm{e}^{itD_\varepsilon} \underline{w} \right), \ \mathbf{x} \in \mathbb{R}^d, \ t > 0, \\ \underline{w}(\mathbf{x}, 0) = v_0(\mathbf{x}). \end{cases} \tag{2.15}$$

Lemma 2.4. *Define* $h(\mathbf{x}, t) = w(\mathbf{x}, t) - \underline{w}(\mathbf{x}, t)$. *Under the assumption that* $\phi_1, \phi_2 \in H^{m_0+2}(\mathbb{R}^d)$, $m_0 > d/2$, *we have*

$$\|h(\cdot, t)\|_{H^{m_0}} \lesssim \varepsilon^2, \quad 0 \le t \le T, \tag{2.16}$$

for some T *independent of* ε *and* $0 < T < T^*$.

Proof. Taking the difference between (2.13) and (2.15), we get

$$\partial_t h(\mathbf{x}, t) = \frac{i\lambda}{8\sqrt{1 - \varepsilon^2 \Delta}} \left[\mathrm{e}^{2it/\varepsilon^2} \mathrm{e}^{-itD_\varepsilon} \left(\mathrm{e}^{itD_\varepsilon} w \right)^3 + \mathrm{e}^{-4it/\varepsilon^2} \mathrm{e}^{-itD_\varepsilon} \left(\mathrm{e}^{-itD_\varepsilon} \overline{w} \right)^3 \right.$$
$$\left. + 3\mathrm{e}^{-2it/\varepsilon^2} \mathrm{e}^{-itD_\varepsilon} \left| \mathrm{e}^{itD_\varepsilon} w \right|^2 \left(\mathrm{e}^{-itD_\varepsilon} \overline{w} \right) + f_h(\mathbf{x}, t) \right], \quad t > 0,$$

with $h(\mathbf{x}, 0) = 0$ and

$$f_h(\mathbf{x}, t) := 3\mathrm{e}^{-itD_\varepsilon} \left[\left| \mathrm{e}^{itD_\varepsilon} w \right|^2 \left(\mathrm{e}^{itD_\varepsilon} w \right) - \left| \mathrm{e}^{itD_\varepsilon} \underline{w} \right|^2 \left(\mathrm{e}^{itD_\varepsilon} \underline{w} \right) \right] = O(h).$$

Hence, the solution reads

$$h(\mathbf{x}, t) = \frac{i\lambda}{8\sqrt{1 - \varepsilon^2 \Delta}} \left[\int_0^t f_h(\mathbf{x}, \theta) d\theta + \int_0^t 3\mathrm{e}^{-2i\theta/\varepsilon^2} \mathrm{e}^{-i\theta D_\varepsilon} \left| \mathrm{e}^{i\theta D_\varepsilon} w \right|^2 \left(\mathrm{e}^{-i\theta D_\varepsilon} \overline{w} \right) d\theta \right.$$
$$\left. + \int_0^t \mathrm{e}^{2i\theta/\varepsilon^2} \mathrm{e}^{-i\theta D_\varepsilon} \left(\mathrm{e}^{i\theta D_\varepsilon} w \right)^3 d\theta + \int_0^t \mathrm{e}^{-4i\theta/\varepsilon^2} \mathrm{e}^{-i\theta D_\varepsilon} \left(\mathrm{e}^{-i\theta D_\varepsilon} \overline{w} \right)^3 d\theta \right].$$

Based on the assumption, we have $v_0 \in H^{m_0+2}$. Therefore from (2.13),

$$\|w(\cdot, t)\|_{H^{m_0+2}} + \|\partial_t w(\cdot, t)\|_{H^{m_0+2}} \lesssim 1, \quad 0 \le t < T,$$

for some $T > 0$. Also note that in the sense of operator, $0 \le D_\varepsilon \le -\Delta/2$. Then for the three integral terms with highly oscillatory phases, by doing the integration-by-parts on the phase, we can get

$$\|h(\cdot, t)\|_{H^{m_0}} \lesssim \varepsilon^2, \quad 0 < t < T,$$

for another $T > 0$ independent of ε. $\qquad\square$

The system (2.15) is the leading order limit model of (2.13). By reversing the transforms, we define

$$u_{CE}(\mathbf{x}, t) := \frac{1}{2} \left[\mathrm{e}^{it/\varepsilon^2 \sqrt{1 - \varepsilon^2 \Delta}} \underline{w}(\mathbf{x}, t) + \mathrm{e}^{-it/\varepsilon^2 \sqrt{1 - \varepsilon^2 \Delta}} \overline{\underline{w}}(\mathbf{x}, t) \right],$$

to get the leading order Chapman-Enskog expansion for KG (1.1) as follows

$$u(\mathbf{x}, t) = u_{CE}(\mathbf{x}, t) + o(1), \quad \varepsilon \to 0.$$

Corollary 2.5. *Define $R(\mathbf{x}, t) = u(\mathbf{x}, t) - u_{CE}(\mathbf{x}, t)$. Under the assumption that $\phi_1, \phi_2 \in H^{m_0+2}(\mathbb{R}^d)$, $m_0 > d/2$, we have*

$$\|R(\cdot, t)\|_{H^{m_0}} \lesssim \varepsilon^2, \quad 0 \le t \le T, \tag{2.17}$$

for some T independent of ε and $0 < T < T^*$.

Proof. By noting

$$u(\mathbf{x}, t) := \frac{1}{2} \left[e^{it/\varepsilon^2 \sqrt{1-\varepsilon^2 \Delta}} w(\mathbf{x}, t) + e^{-it/\varepsilon^2 \sqrt{1-\varepsilon^2 \Delta}} w(\mathbf{x}, t) \right], \quad \mathbf{x} \in \mathbb{R}^d, \ t \ge 0,$$

it becomes obvious from Lemma 2.4. □

Comparison of Modulated Fourier Expansion (MFo), the Multiscale Frequency Expansion (MFe) and Chapman-Enkog expansion (CE): In contrast to the modulated Fourier expansion (2.1) and the multiscale expansion by frequency (2.10), the Chapman-Enkog expansion (2.15) incorporates more higher order corrections into the limit model. Therefore, though all the three expansions converge quadratically in ε, one would expect the Chapman-Enskog expansion (2.15) being closer to the solution of KG in the nonrelativistic limit regime.

The drawback is however that (2.15) involves the evaluation of the pseudo-differential operation for several times, which is more expensive than solving (2.1) or (2.10) in practical computing. (Note that the limit equation (2.15) can be solved for instance with a finite difference time integration scheme.) When the whole space KG equation (1.1) is truncated onto a periodic domain or zero-boundary domain, those pseudo-differential operations can be computed by FFT quite efficiently. However, if the KG equation is imposed on a general domain, spatial approximations for (2.15) are not easily obtained.

2.4. **Dynamics and comparisons.** In this section, we consider the KG (1.1) in one space dimension ($d = 1$, $\mathbf{x} = x$). As a reference solution we employ the uniformly accurate method [7] with a very small step size to obtain a very accurate approximation to the solution $u(x, t)$ under different $0 < \varepsilon \le 1$.

As we are interested in the comparison of the asymptotic error introduced under the different expansion techniques we solve the corresponding limit model of each expansion accurately by proper numerical methods as discussed before. We study and compare the three presented expansions by the size of the remainders at a fixed time and the dynamics of the remainders. For simplicity, we refer to the modulated Fourier expansion by MFo, the multiscale frequency expansion by MFe and the Chapman-Enskog expansion by CE. We denote the remainder of each as R_{MFo}, R_{MFe} and R_{CE}.

Example 2.6 (Comparison in accuracy)**.** We begin with the comparison of the accuracy of each expansion at a fixed time under different ε. We choose the following initial value in (1.1)

$$u(x, 0) = \frac{sech(x^2)}{2}, \quad \partial_t u(x, 0) = \frac{e^{-x^2}}{2}, \quad x \in \mathbb{R} \tag{2.18}$$

and compute the remainder of the MFo, MFe and CE expansions presented above. The remainders R_{MFo} R_{MFe} and R_{CE} measured in a discrete H^1-norm at $T = 0.5$

TABLE 2. Remainders (in H^1-norm) of the leading order modu-
lated Fourier (MFo) expansion, the multiscale expansion by fre-
quency (MFe) and the Chapman-Enskog (CE) expansion.

$t = 0.5$	$\varepsilon = 0.1$	$\varepsilon/2$	$\varepsilon/2^2$	$\varepsilon/2^3$
MFo	3.46E-2	9.90E-3	2.60E-3	6.50E-4
MFe	1.00E-2	2.10E-3	5.35E-4	1.31E-4
CE	1.20E-3	2.58E-4	6.59E-5	1.79E-5
$t = 1$	$\varepsilon = 0.1$	$\varepsilon/2$	$\varepsilon/2^2$	$\varepsilon/2^3$
MFo	6.15E-2	1.88E-2	5.00E-3	1.30E-3
MFe	9.70E-3	2.40E-3	5.94E-4	1.51E-4
CE	9.29E-4	2.87E-4	7.23E-5	1.74E-5

and $T = 1$ are shown in Table 2. The quadratic convergence rate in ε of the
three expansions is clearly justified in the numerical experiments. Furthermore, as
presumed, the CE expansion allows the closest approximation to the solution of
KG in the nonrelativistic limit regime (introducing the smallest error).

Example 2.7 (Dynamics of remainders). We compute the dynamics of the re-
mainder term of the each expansion. Firstly, we consider the one-dimensional KG
equation (1.1) with smooth initial data in two cases: Once we choose an initially
localized wave in the whole space $\mathbb{R}$, i.e., (2.18). In the other case we choose a
planewave on a 2π-torus $\mathbb{T}$, i.e.,

$$\phi_1(x) = \frac{2\cos(x)}{\sqrt{3}}, \quad \phi_2(x) = \frac{\sin(x) + 2\cos(x)}{2}, \quad x \in \mathbb{T}. \qquad (2.19)$$

We simulate the dynamics of the remainder terms R_{MFo}, R_{MFe} and R_{CE} under the
three expansions for the above two cases (2.18) and (2.19). Their behavior in the
H^1-norm divided by ε^2 is plotted in Figure 2. The profiles given by the expansions
u_{MFo}, u_{MFe} and u_{CE} as approximations to the solution of the KG $u(x, t)$ at time
$t = 3$ are plotted in Figure 3.

The numerical results demonstrate the following: 1) The remainders of all the
expansions retain at order $O(\varepsilon^2)$ within the $O(1)$ time scale. 2) In the whole space
case, MFo has a (linearly) increasing remainder with respect to time, while the
remainders of MFe and CE are $O(\varepsilon^2)$ uniformly in time. 3) In the case of the torus,
all the expansions lead to an increasing remainder, whereby the remainders of MFe
and CE start to increase only after some time (after $t = 1$ from the figure).

Example 2.8 (Energy conservation). Under the cubic nonlinearity (1.2), one of
the most important conserved physical quantity of the KG equation is the energy
or Hamiltonian:

$$H(t) := \int_{\mathbb{R}^d} \left[\varepsilon^2 (\partial_t u)^2 + |\nabla u|^2 + \frac{1}{\varepsilon^2} u^2 + \frac{\lambda}{2} u^4 \right] d\mathbf{x} \equiv H(0), \quad t \geq 0.$$

We compute the approximated energy $\mathcal{H}(t)$ by using the three leading order ex-
pansions of u. Note that the exact energy $H(0)$ is given exactly from the initial
data. The relative energy error $|\mathcal{H}(t) - H(0)|/|H(0)|$ as a function of time in the
case of the whole space (2.18) and torus (2.19), respectively, is plotted in Figure
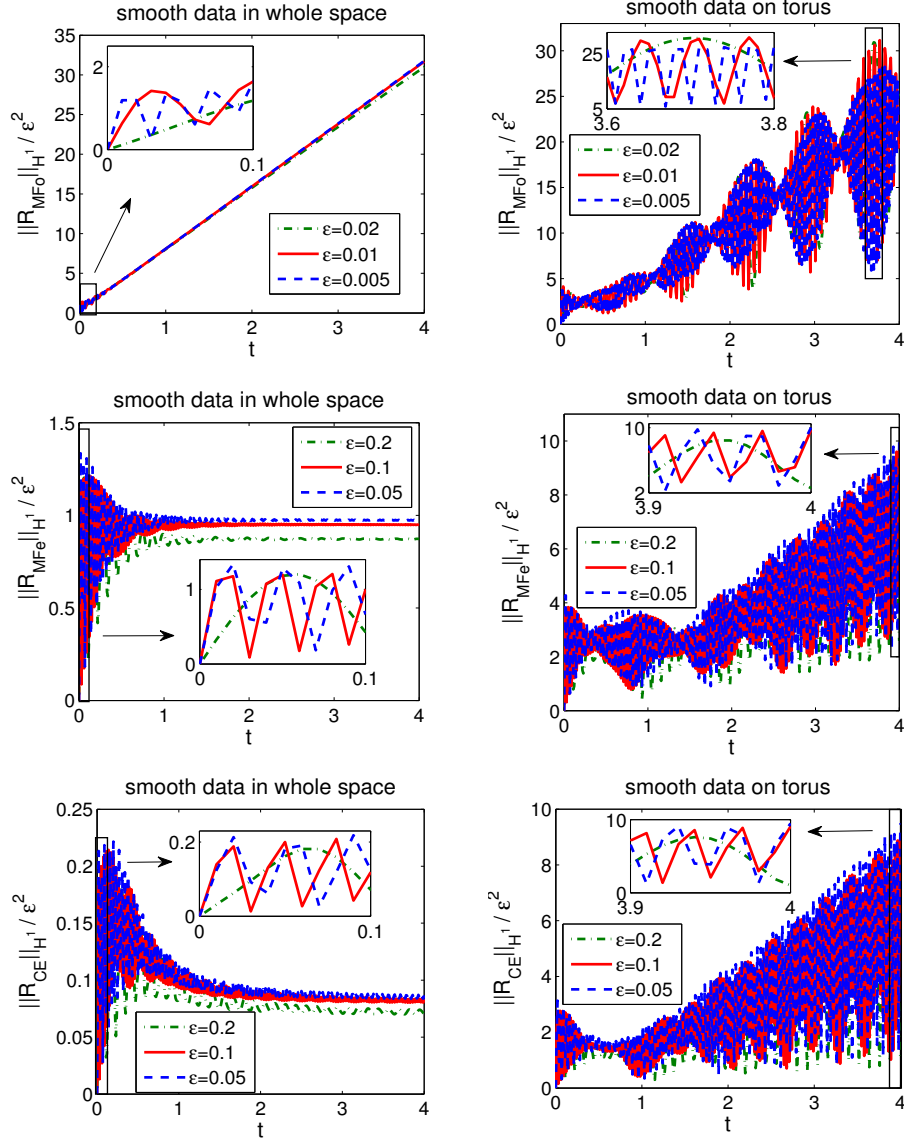4. The results show that the errors in the energy converges relatively with rate

FIGURE 2. Behavior of the remainder terms $\|R_{MFo}\|_{H^1}/\varepsilon^2$, $\|R_{MFe}\|_{H^1}/\varepsilon^2$ and $\|R_{CE}\|_{H^1}/\varepsilon^2$ with respect to time under two cases: initial smooth localized wave (2.18) in $\mathbb{R}$ (left) and smooth planewave (2.19) on torus $\mathbb{T}$ (right).

$O(\varepsilon^2)$. Moreover, the energy error of the three expansions appears to be uniformly bounded in time.

Example 2.9 (Comparison in regularity). Next, we numerically investigate the behavior of the remainders under non-smooth initial data. By doing so, we are
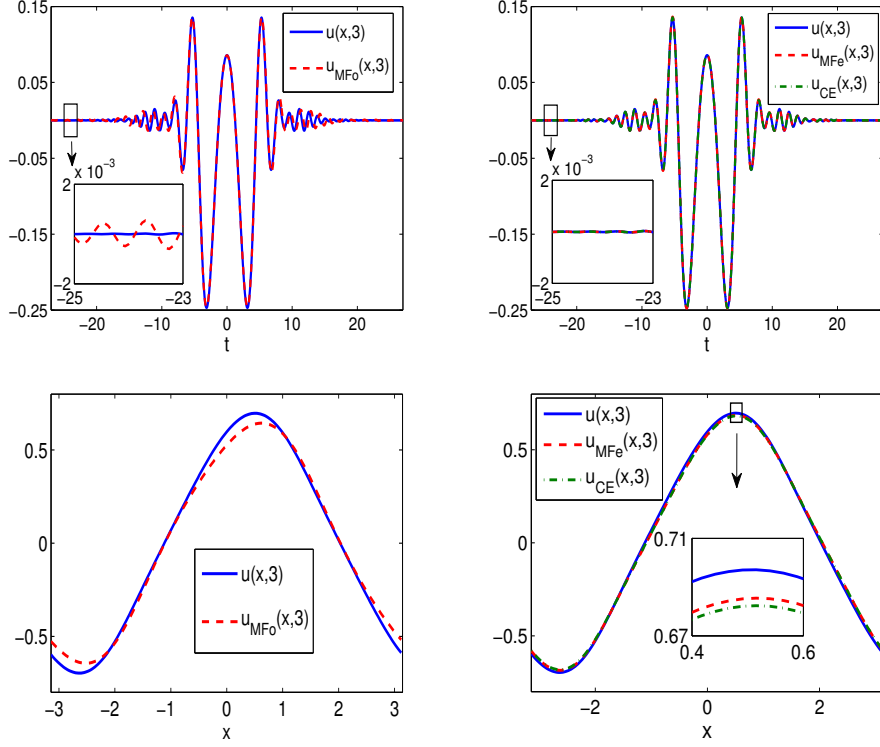
FIGURE 3. Profiles of the expansions $u_{MFo}(x,3)$, $u_{MFe}(x,3)$, $u_{CE}(x,3)$ and exact solution $u(x,3)$ at $t = 3$ under $\varepsilon = 0.1$: the whole space example (2.18) (up) and the torus example (2.19) (down).

aiming to justify the critical regularity requirement of each expansion as given in the Lemmas 2.1-2.4. In the case of the torus, we follow the construction in [27] to obtain the low regularity initial data. More precisely, we choose in KG (1.1)

$$\phi_1(x) = \frac{\sqrt{2}|\partial_{x,N}|^{-\theta}\mathcal{U}^N}{\||\partial_{x,N}|^{-\theta}\mathcal{U}^N\|_{L^\infty}}, \quad \phi_2(x) = \frac{\sqrt{2}|\partial_{x,N}|^{-\theta}\mathcal{U}^N}{\||\partial_{x,N}|^{-\theta}\mathcal{U}^N\|_{L^\infty}}, \quad x \in \mathbb{T}, \qquad (2.20)$$

where N is an even integer, $\mathcal{U}^N \in [0,1]^N$ is a uniformly distributed random vector and the pseudo-differential operator $|\partial_{x,N}|^{-\theta}$ with $\theta \geq 0$ reads for Fourier modes $k = -N/2, \ldots N/2 - 1$,

$$\left(|\partial_{x,N}|^{-\theta}\right)_k := \begin{cases} |k|^{-\theta} & \text{if } k \neq 0, \\ 0 & \text{if } k = 0. \end{cases}$$

Apparently, we can choose θ such that the data $\phi_1, \phi_2 \in H^\theta(\mathbb{T})$. For the modulated Fourier expansion, we choose $\theta = 5$ and 4, respectively, and measure the remainder in the discrete H^1-norm and L^2-norm. For the multiscale expansion by frequency or the Chapman-Enskog expansion, we choose the critical values for θ as 3 and 2, respectively. The results are plotted in Figures 5-7.
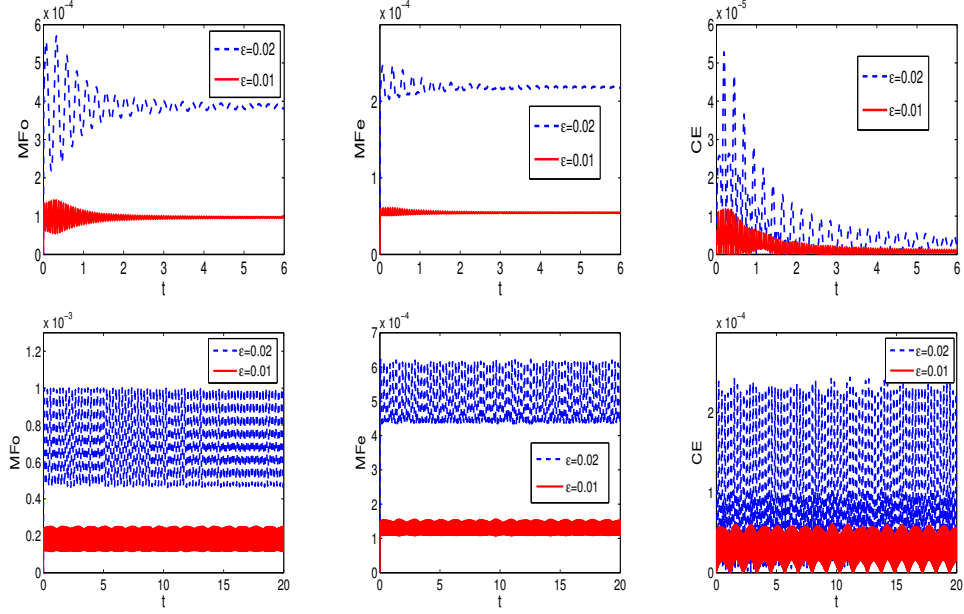
FIGURE 4. Energy error $|\mathcal{H}(t) - H(0)|/|H(0)|$ of the three expansions to the leading order under whole space case (up) and torus case (down).
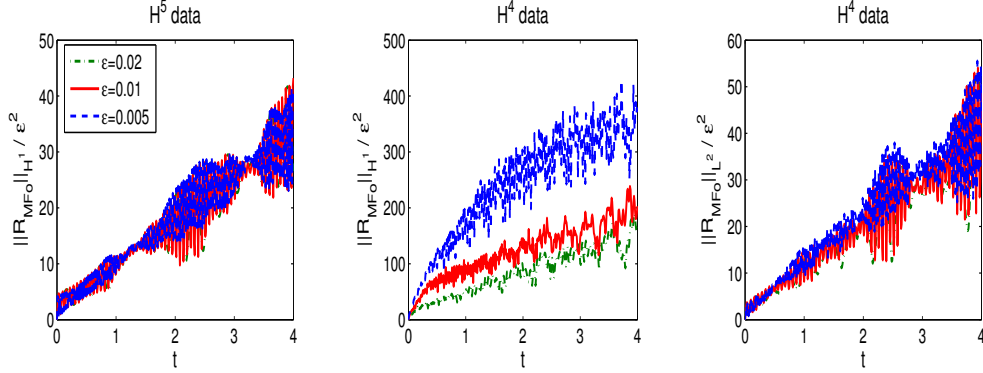

FIGURE 5. Behavior of the MFo remainder under lower regularity initial data (2.20): $\|R_{MFo}\|_{H^1}/\varepsilon^2$ (left) under H^5-data, $\|R_{MFo}\|_{H^1}/\varepsilon^2$ (middle) and $\|R_{MFo}\|_{L^2}/\varepsilon^2$ (right) under H^4-data.

From the results, we can see: 1) H^{m_0+4} regularity requirement of the initial data is critical for MFo to allow the quadratic convergence $\|R_{MFo}\|_{H^{m_0}} = O(\varepsilon^2)$. 2) H^{m_0+2}-initial data is critical for MFe and CE to allow $\|R_{MFo}\|_{H^{m_0}}, \|R_{CE}\|_{H^{m_0}} = O(\varepsilon^2)$.
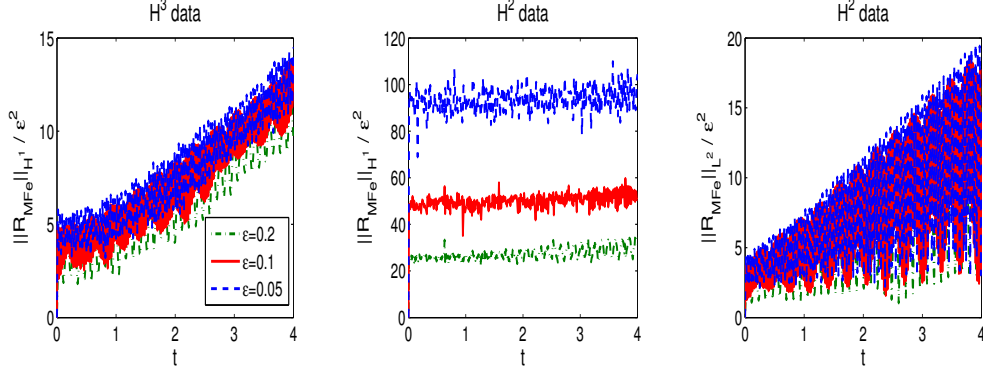
FIGURE 6. Behavior of the MFe remainder under lower regularity initial data (2.20): $\|R_{MFe}\|_{H^1}/\varepsilon^2$ (left) under H^3-data, $\|R_{MFe}\|_{H^1}/\varepsilon^2$ (middle) and $\|R_{MFe}\|_{L^2}/\varepsilon^2$ (right) under H^2-data.
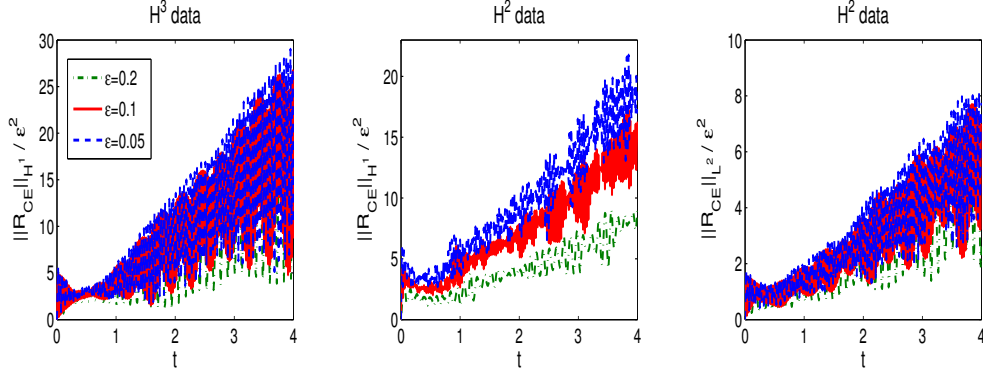

FIGURE 7. Behavior of the CE remainder under lower regularity initial data (2.20): $\|R_{CE}\|_{H^1}/\varepsilon^2$ (left) under H^3-data, $\|R_{CE}\|_{H^1}/\varepsilon^2$ (middle) and $\|R_{CE}\|_{L^2}/\varepsilon^2$ (right) under H^2-data.

3. NEXT ORDER EXPANSION

In this section, we present the higher order version of the discussed expansions.

3.1. Modulated Fourier expansion.

Here we shall adopt the notations introduced in Section 2.1. The modulated Fourier expansion of the solution of KG (1.1) were found in [19] up to the next order term as follows

$$u(\mathbf{x}, t) = e^{it/\varepsilon^2} z(\mathbf{x}, t) + e^{-it/\varepsilon^2} \overline{z}(\mathbf{x}, t) + \varepsilon^2 w(\mathbf{x}, t) + o(\varepsilon^2), \quad \mathbf{x} \in \mathbb{R}^d, \quad t \geq 0,$$

where $w := w(\mathbf{x}, t) \in \mathbb{R}$ satisfies

$$w(\mathbf{x}, t) = v(\mathbf{x}, t)\mathrm{e}^{it/\varepsilon^2} + \overline{v}(\mathbf{x}, t)\mathrm{e}^{-it/\varepsilon^2} + \frac{\lambda}{8}\left[z(\mathbf{x}, t)^3\mathrm{e}^{3it/\varepsilon^2} + \overline{z}(\mathbf{x}, t)^3\mathrm{e}^{-3it/\varepsilon^2}\right]$$
$$- \frac{3\lambda}{4}|z(\mathbf{x}, t)|^2\left[z(\mathbf{x}, t)\mathrm{e}^{it/\varepsilon^2} + \overline{z}(\mathbf{x}, t)\mathrm{e}^{-it/\varepsilon^2}\right], \quad \mathbf{x} \in \mathbb{R}^d, \quad t \geq 0.$$

Thereby, $z := z(\mathbf{x}, t)$ solves the NLS system (2.2) and $v := v(\mathbf{x}, t)$ solves an additional NLS-type equation

$$\begin{cases} 2i\partial_t v - \Delta v + 6\lambda|z|^2 v + 3\lambda(z)^2\overline{v} = \frac{1}{4}\Delta^2 z + \frac{51\lambda^2}{8}|z|^4 z - \frac{3\lambda}{2}\Delta(|z|^2 z), \ t \geq 0, \\ v(\mathbf{x}, 0) = -\frac{\lambda}{4}z(\mathbf{x}, 0)^3 + \frac{\lambda}{8}\overline{z}(\mathbf{x}, 0)^3 + \frac{3\lambda}{4}|z(\mathbf{x}, 0)|^2\overline{z}(\mathbf{x}, 0) + \frac{1}{4}\Delta(z(\mathbf{x}, 0) - \overline{z}(\mathbf{x}, 0)). \end{cases}$$
$$(3.1)$$

The convergence from $u(\mathbf{x}, t)$ to $u_{MFo}(\mathbf{x}, t)$

$$u_{MFo}(\mathbf{x}, t) = \mathrm{e}^{it/\varepsilon^2} z(\mathbf{x}, t) + \mathrm{e}^{-it/\varepsilon^2}\overline{z}(\mathbf{x}, t) + \varepsilon^2 w(\mathbf{x}, t)$$

as $\varepsilon \to 0$ is given as follows.

Lemma 3.1. *Define $r(\mathbf{x}, t) = u(\mathbf{x}, t) - u_{MFo}(\mathbf{x}, t)$. Under the assumption that $\phi_1, \phi_2 \in H^{m_0+8}(\mathbb{R}^d)$, $m_0 > d/2$, we have*

$$\|r(\cdot, t)\|_{H^{m_0}} \lesssim \varepsilon^4, \quad 0 \leq t \leq T, \tag{3.2}$$

for some T independent of ε and $0 < T < T^*$.

Remark 3.2. Again we give a new (shorter) proof of the general result obtained in [19] for the fourth order correction ε^4. Again our regularity assumptions on the solution go in line with [19, Theorem 2] (with $\varepsilon = c^{-1}$).

Proof of Lemma 3.1. Based the leading order expansion (2.3) and the remainder equation for R (2.5), now we compute each term with $R = \varepsilon^2 w + r$. For the initial data of r, we find

$$r(\mathbf{x}, 0) = -\varepsilon^2 w(\mathbf{x}, 0) = -\varepsilon^2\left(v(\mathbf{x}, 0) + \frac{\lambda}{8}z(\mathbf{x}, 0)^3 - \frac{3\lambda}{4}|z(\mathbf{x}, 0)|^2 z(\mathbf{x}, 0) + c.c.\right) = 0.$$

For the initial derivative of r, we have

$$\partial_t r(\mathbf{x}, 0) = \partial_t R(\mathbf{x}, 0) - \varepsilon^2\partial_t w(\mathbf{x}, 0)$$
$$= \varepsilon^2\partial_t v(\mathbf{x}, 0) + \varepsilon^2\frac{\lambda}{8}\partial_t(z^3)(\mathbf{x}, 0) - \varepsilon^2\frac{3\lambda}{4}\partial_t(|z|^2 z)(\mathbf{x}, 0) + c.c. =: \varepsilon^2\gamma(\mathbf{x}),$$

where $\gamma \in H^{m_0+2}$. Now let us firstly check the time derivative term in the equation (2.5). We have

$$\varepsilon^2\partial_{tt}R = \varepsilon^4\partial_{tt}w + \varepsilon^2\partial_{tt}r,$$

with

$$\varepsilon^4\partial_{tt}w = \varepsilon^2\mathrm{e}^{it/\varepsilon^2}2i\partial_t v - \mathrm{e}^{it/\varepsilon^2}v - \mathrm{e}^{3it/\varepsilon^2}\frac{9\lambda}{8}z^3 + \varepsilon^2\mathrm{e}^{3it/\varepsilon^2}\frac{6i\lambda}{8}\partial_t(z^3) + \mathrm{e}^{it/\varepsilon^2}\frac{3\lambda}{4}|z|^2 z$$
$$- \varepsilon^2\mathrm{e}^{it/\varepsilon^2}\frac{3i\lambda}{2}\partial_t(|z|^2 z) + c.c. + \varepsilon^4 O(\partial_{tt}v) + \varepsilon^4 O(\partial_{tt}z).$$

Next, we compute the nonlinear term f_R:

$$f_R = \varepsilon^2 6\lambda |z|^2 w + \varepsilon^2 \mathrm{e}^{2it/\varepsilon^2} 3\lambda z^2 w + \varepsilon^2 \mathrm{e}^{-2it/\varepsilon^2} 3\lambda \overline{z}^2 w + \varepsilon^4 O(w^2) + O(r)$$

$$=\varepsilon^2 \mathrm{e}^{it/\varepsilon^2} 6\lambda |z|^2 v - \varepsilon^2 \mathrm{e}^{it/\varepsilon^2} \frac{51\lambda^2}{8}|z|^4 z + \varepsilon^2 \mathrm{e}^{it/\varepsilon^2} 3\lambda z^2 \overline{v} + c.c. + \varepsilon^2 g + \varepsilon^4 O(w^2) + O(r),$$

with

$$g = \mathrm{e}^{3it/\varepsilon^2} \frac{3\lambda^2}{4}|z|^2 z^3 + \mathrm{e}^{3it/\varepsilon^2} 3\lambda z^2 \left[v - \frac{3\lambda}{4}|z|^2 z\right] + \mathrm{e}^{5it/\varepsilon^2} \frac{3\lambda^2}{8} z^5 w + c.c..$$

Then together with

$$-\Delta R + \frac{R}{\varepsilon^2} = -\varepsilon^2 \mathrm{e}^{it/\varepsilon^2} \Delta v + \varepsilon^2 \mathrm{e}^{it/\varepsilon^2} \frac{3\lambda}{4} \Delta \left(|z|^2 z\right) + \varepsilon^2 \mathrm{e}^{3it/\varepsilon^2} \frac{\lambda}{8} \Delta z^3$$

$$+ \mathrm{e}^{it/\varepsilon^2} v - \mathrm{e}^{it/\varepsilon^2} \frac{3\lambda}{4}|z|^2 z + \mathrm{e}^{3it/\varepsilon^2} \frac{\lambda}{8} z^3 + c.c. - \Delta r + \frac{r}{\varepsilon^2},$$

and noting (3.1) and

$$\partial_{tt} z = \frac{1}{4}\left[-\Delta^2 z + 3\lambda \Delta \left(|z|^2 z\right)\right] + \frac{3i\lambda}{2}\partial_t \left(|z|^2 z\right),$$

the equation (2.5) becomes

$$\begin{cases} \varepsilon^2 \partial_{tt} r - \Delta r + \frac{r}{\varepsilon^2} + \varepsilon^4 O(\partial_{tt}v) + \varepsilon^4 O(\partial_{tt}z) + \varepsilon^2 \tilde{g} + \varepsilon^4 O(w^2) + O(r) = 0, \\ r(\mathbf{x},0) = 0, \quad \partial_t r(\mathbf{x},0) = \varepsilon^2 \gamma(\mathbf{x}), \end{cases} \quad (3.3)$$

with

$$\tilde{g} = \mathrm{e}^{3it/\varepsilon^2} \frac{6i\lambda}{8} \partial_t(z^3) + \mathrm{e}^{3it/\varepsilon^2} \frac{\lambda}{8} \Delta z^3 + c.c. + g.$$

By the regularity assumption, we have $z(\mathbf{x},t) \in H^{m_0+8}$. Hence, from equation (3.1), we find $v \in H^{m_0+4}$ and $\partial_{tt}v \in H^{m_0}$. Therefore, by standard techniques, we can get $\|r\|_{H^{m_0}} \lesssim \varepsilon^4$. $\qquad \square$

3.2. **Multiscale expansion by frequency.** The high order multiscale expansion by frequency of the solution $u = u(\mathbf{x},t)$ of the KG (1.1) has recently been described in [10]:

$$u(\mathbf{x},t) = \mathrm{e}^{it/\varepsilon^2} z^\varepsilon(\mathbf{x},t) + \frac{\varepsilon^2 \lambda}{8} \mathrm{e}^{3it/\varepsilon^2} z^\varepsilon(\mathbf{x},t)^3 + c.c. + o(\varepsilon^2), \quad \mathbf{x} \in \mathbb{R}^d, \ t \geq 0, \ (3.4)$$

where $z^\varepsilon = z^\varepsilon(\mathbf{x},t)$ satisfying

$$\begin{cases} 2i\partial_t z^\varepsilon + \varepsilon^2 \partial_{tt} z^\varepsilon - \Delta z^\varepsilon + 3\left(\lambda |z^\varepsilon|^2 + \frac{\varepsilon^2 \lambda^2}{8}|z^\varepsilon|^4\right) z^\varepsilon = 0, \ \mathbf{x} \in \mathbb{R}^d, \ t > 0, \ (3.5) \\ z^\varepsilon(\mathbf{x},0) = w_0(\mathbf{x}) + \varepsilon^2 r_0(\mathbf{x}), \quad \partial_t z^\varepsilon(\mathbf{x},0) = \frac{i}{2}\left(-\Delta w_0(\mathbf{x}) + 3\lambda |w_0(\mathbf{x})|^2 w_0(\mathbf{x})\right), \end{cases}$$

with

$$w_0(\mathbf{x}) = \frac{1}{2}(\phi_1(\mathbf{x}) - i\phi_2(\mathbf{x})), \quad r_0(\mathbf{x}) = \frac{\lambda}{8}\overline{w}_0(\mathbf{x})^3 - \frac{\lambda}{4}w_0(\mathbf{x})^3 + \frac{3i\lambda}{4}|w_0|^2 \phi_2 - \frac{i}{4}\Delta \phi_2.$$

The expansion

$$u_{MFe}(\mathbf{x},t) = \mathrm{e}^{it/\varepsilon^2} z^\varepsilon(\mathbf{x},t) + \frac{\varepsilon^2 \lambda}{8} \mathrm{e}^{3it/\varepsilon^2} z^\varepsilon(\mathbf{x},t)^3 + c.c., \quad (3.6)$$

has following short time estimate [10].

Lemma 3.3. *Let $R(\mathbf{x}, t) := u(\mathbf{x}, t) - u_{MFe}(\mathbf{x}, t)$, under the assumption that $\phi_1, \phi_2 \in H^{m_0+5}(\mathbb{R}^d)$, $m_0 > d/2$, we have the following prior estimate on the solution*

$$\|R(\cdot, t)\|_{H^{m_0}} \lesssim \varepsilon^4, \quad 0 \leq t \leq T, \tag{3.7}$$

for some T independent of ε and $0 < T < T^*$.

Proof. See detailed proof in [10]. □

Compared to the modulated Fourier expansion, the above high order multiscale frequency expansion (3.6) is more compact, since it only involves one limit equation, i.e. (3.5) to solve. It allows high order asymptotic convergence in ε^4 by absorbing some corrections to the limit model. The limit model (3.5) can again be numerically solved by exponential integrators.

3.3. **Chapman-Enskog expansion.** The high order version of the Chapman-Enskog expansion presented below is introduced by Mohammed Lemou et al, and it has been utilised to design uniformly accurate scheme in [13].

Recall the formulation (2.14). The expansion of $w(\mathbf{x}, t)$ reads

$$w(\mathbf{x}, t) = \underline{w}(\mathbf{x}, t) + \varepsilon^2 \Theta(t, t/\varepsilon^2, \underline{w}(\mathbf{x}, t)) + o(\varepsilon^2), \quad \varepsilon \to 0,$$

where

$$\Theta(t, \xi, \underline{w}) := (I - \Pi) \int_0^\xi [F(t, \theta, \underline{w}) - \Pi F(t, \cdot, \underline{w})] \, d\theta, \tag{3.8}$$

and $\underline{w} = \underline{w}(\mathbf{x}, t)$ solves

$$\begin{cases} \partial_t \underline{w} = \dfrac{1}{2\pi} \displaystyle\int_0^{2\pi} F(t, \xi, \underline{w} + \varepsilon^2 \Theta(t, \xi, \underline{w})) \, d\xi, \\ \underline{w}(\mathbf{x}, 0) = v_0(\mathbf{x}) - \varepsilon^2 \Theta(0, 0, v_0(\mathbf{x})). \end{cases} \tag{3.9}$$

Due to our cubic nonlinearity, one can explicitly obtain that

$$\Theta(t, \xi, \underline{w}) = \frac{\lambda}{16\sqrt{1 - \varepsilon^2 \Delta}} \left[e^{2i\xi} e^{-itD_\varepsilon} \left(e^{itD_\varepsilon} \underline{w} \right)^3 - 3e^{-2i\xi} e^{-itD_\varepsilon} \left| e^{itD_\varepsilon} \underline{w} \right|^2 e^{-itD_\varepsilon} \overline{\underline{w}} \right.$$
$$\left. - \frac{1}{2} e^{-4i\xi} \left(e^{-itD_\varepsilon} \overline{\underline{w}} \right)^3 \right]. \tag{3.10}$$

Denote

$$\rho_0 = e^{itD_\varepsilon} \underline{w}, \quad \rho_1 = \frac{-3\varepsilon^2 \lambda}{16\sqrt{1 - \varepsilon^2 \Delta}} \left| e^{itD_\varepsilon} \underline{w} \right|^2 e^{-itD_\varepsilon} \overline{\underline{w}},$$

$$\rho_2 = \frac{\varepsilon^2 \lambda}{16\sqrt{1 - \varepsilon^2 \Delta}} \left(e^{itD_\varepsilon} \underline{w} \right)^3, \quad \rho_3 = \frac{-\varepsilon^2 \lambda}{32\sqrt{1 - \varepsilon^2 \Delta}} \left(e^{-itD_\varepsilon} \overline{\underline{w}} \right)^3.$$

The limit equation (3.9) for $\underline{w}$ can be written explicitly down as

$$\partial_t \underline{w} = \frac{i\lambda}{8\sqrt{1 - \varepsilon^2 \Delta}} \left[3g_0 + 3g_1 + g_2 + g_3 \right],$$

where

$$g_0 = |\rho_0|^2 \rho_0 + 2|\rho_2|^2 \rho_0 + 2\overline{\rho}_0 \rho_1 \rho_2 + 2\rho_0 |\rho_1|^2 + 2\rho_2 \overline{\rho}_1 \rho_3 + \rho_1^2 \overline{\rho}_3 + 2\rho_0 |\rho_3|^2,$$

$$g_1 = \overline{\rho}_0^2 \rho_2 + 2|\rho_0|^2 \overline{\rho}_1 + 2\overline{\rho}_1 |\rho_2|^2 + |\rho_1|^2 \overline{\rho}_1 + 2\rho_0 \overline{\rho}_2 \overline{\rho}_3 + 2\overline{\rho}_0 \rho_1 \overline{\rho}_3 + 2\overline{\rho}_1 |\rho_3|^2,$$

$$g_2 = 3\rho_0^2 \rho_1 + 3\rho_1^2 \rho_2 + 6\rho_0 \rho_2 \rho_3, \quad g_3 = 3\overline{\rho}_1^2 \overline{\rho}_0 + 3(\overline{\rho}_0)^2 \overline{\rho}_3 + 6\overline{\rho}_1 \overline{\rho}_2 \overline{\rho}_3.$$

Lemma 3.4. *Define* $h(\mathbf{x}, t) = w(\mathbf{x}, t) - \underline{w}(\mathbf{x}, t) - \varepsilon^2 \Theta(t, t/\varepsilon^2, \underline{w}(\mathbf{x}, t))$. *Under the assumption that* $\phi_1, \phi_2 \in H^{m_0+4}(\mathbb{R}^d)$, $m_0 > d/2$, *we have*

$$\|h(\cdot, t)\|_{H^{m_0}} \lesssim \varepsilon^4, \quad 0 \le t \le T, \tag{3.11}$$

for some T *independent of* ε *and* $0 < T < T^*$.

Proof. In this case the explicit formulas are lengthy. For reasons of ease and clarity of presentation we will not carry out the proof with detailed terms as we did in Lemma 2.4. Instead, we will write things in an abstract form.

Firstly, we verify (3.11) at initial time.

$$\begin{aligned}
h(\mathbf{x}, 0) &= w(\mathbf{x}, 0) - \underline{w}(\mathbf{x}, 0) - \varepsilon^2 \Theta(0, 0, \underline{w}(\mathbf{x}, 0)) \\
&= \varepsilon^2 \left[\Theta\left(0, 0, v_0(\mathbf{x})\right) - \Theta\left(0, 0, \underline{w}(\mathbf{x}, 0)\right) \right] \\
&= \varepsilon^4 \int_0^1 \nabla \Theta\left(0, 0, v_0(\mathbf{x}) - \theta \varepsilon^2 \Theta(0, 0, v_0(\mathbf{x}))\right) \Theta(0, 0, v_0(\mathbf{x})) d\theta
\end{aligned}$$

where we denote $\nabla \Theta(t, \xi, w) = \partial_w \Theta(t, \xi, w)$. With $v_0 \in H^{m_0+4}$, we have

$$\|h(\cdot, 0)\|_{H^{m_0+4}(\mathbb{R}^d)} \lesssim \varepsilon^4.$$

By the regularity assumption, one has for the limit model:

$$\partial_t^k \underline{w}(\mathbf{x}, t) \in H^{m_0+4-2k}(\mathbb{R}^d), \quad k = 0, 1, 2, \quad 0 \le t \le T,$$

for some $T > 0$.

Now for simplicity of notation, we would drop the space variable $\mathbf{x}$. By differentiation, we get

$$\begin{aligned}
\partial_t h =& F(t, t/\varepsilon^2, w) - \Pi F\left(t, \cdot, \underline{w} + \varepsilon^2 \Theta(t, \cdot, \underline{w})\right) - \varepsilon^2 \partial_t \Theta(t, t/\varepsilon^2, \underline{w}) - \partial_\xi \Theta(t, t/\varepsilon^2, \underline{w}) \\
& - \varepsilon^2 \nabla \Theta\left(t, t/\varepsilon^2, \underline{w}\right) \partial_t \underline{w}, \quad t > 0.
\end{aligned} \tag{3.12}$$

By (3.8), we find

$$\partial_\xi \Theta(t, \xi, \underline{w}) = F(t, \xi, \underline{w}) - \Pi F(t, \cdot, \underline{w}).$$

By Taylor's expansion, we get

$$\begin{aligned}
&\Pi F\left(t, \cdot, \underline{w} + \varepsilon^2 \Theta(t, \cdot, \underline{w})\right) \\
&= \Pi F(t, \cdot, \underline{w}) + \varepsilon^2 \Pi \int_0^1 \nabla F\left(t, \cdot, \underline{w} + \theta \varepsilon^2 \Theta(t, \cdot, \underline{w})\right) \Theta(t, \cdot, \underline{w}) d\theta,
\end{aligned}$$

and

$$\begin{aligned}
F(t, t/\varepsilon^2, w) =& F(t, t/\varepsilon^2, \underline{w}) + \int_0^1 \nabla F\left(t, t/\varepsilon^2, \underline{w} + \theta(\varepsilon^2 \Theta + h)\right) (\varepsilon^2 \Theta + h) d\theta \\
=& F(t, t/\varepsilon^2, \underline{w}) + \int_0^1 \nabla F\left(t, t/\varepsilon^2, \underline{w} + \theta \varepsilon^2 \Theta\right) (\varepsilon^2 \Theta + h) d\theta \\
& + \int_0^1 \int_0^1 \nabla^2 F\left(t, t/\varepsilon^2, \underline{w} + \theta(\varepsilon^2 \Theta + \sigma h)\right) \theta h(\varepsilon^2 \Theta + h) d\sigma d\theta.
\end{aligned}$$

Denote

$$\begin{aligned}
F_{[h]}(t, \xi) :=& \int_0^1 \nabla F\left(t, \xi, \underline{w}(t) + \theta \varepsilon^2 \Theta\right) h(t) \, d\theta \\
& + \int_0^1 \int_0^1 \nabla^2 F\left(t, \xi, \underline{w}(t) + \theta(\varepsilon^2 \Theta + \sigma h(t))\right) \theta h(t) (\varepsilon^2 \Theta + h(t)) d\sigma d\theta.
\end{aligned}$$

with $\Theta = \Theta(t, \xi, \underline{w}(t))$, then we have

$$F(t, t/\varepsilon^2, w) = F(t, t/\varepsilon^2, \underline{w}) + \varepsilon^2 \int_0^1 \nabla F\left(t, t/\varepsilon^2, \underline{w} + \theta\varepsilon^2\Theta(t, t/\varepsilon^2, \underline{w})\right) \Theta(t, t/\varepsilon^2, \underline{w}) d\theta$$
$$+ F_{[h]}(t, t/\varepsilon^2).$$

Therefore, we find

$$F(t, t/\varepsilon^2, w) - \Pi F\left(t, \cdot, \underline{w} + \varepsilon^2\Theta(t, \cdot, \underline{w})\right) - \partial_\xi \Theta(t, t/\varepsilon^2, \underline{w})$$

$$= \varepsilon^2 \int_0^1 \nabla F\left(t, t/\varepsilon^2, \underline{w} + \theta\varepsilon^2\Theta(t, t/\varepsilon^2, \underline{w})\right) \Theta(t, t/\varepsilon^2, \underline{w}) d\theta + F_{[h]}(t, t/\varepsilon^2)$$

$$- \varepsilon^2 \Pi \int_0^1 \nabla F\left(t, \cdot, \underline{w} + \theta\varepsilon^2\Theta(t, \cdot, \underline{w})\right) \Theta(t, \cdot, \underline{w}) d\theta$$

Denote

$$G(t, \xi) := \int_0^1 \nabla F\left(t, \xi, \underline{w}(t) + \theta\varepsilon^2\Theta(t, \xi, \underline{w}(t))\right) \Theta(t, \xi, \underline{w}(t)) d\theta - \nabla\Theta\left(t, \xi, \underline{w}(t)\right) \partial_t \underline{w}(t)$$

$$- \Pi \int_0^1 \nabla F\left(t, \cdot, \underline{w}(t) + \theta\varepsilon^2\Theta(t, \cdot, \underline{w}(t))\right) \Theta(t, \cdot, \underline{w}(t)) d\theta - \partial_t\Theta(t, \xi, \underline{w}(t)),$$

and then we can write (3.12) as

$$\partial_t h(t) = \varepsilon^2 G(t, t/\varepsilon^2) + F_{[h]}(t, t/\varepsilon^2), \quad t > 0.$$

Now we consider a function $H(t, \xi)$ that solves

$$\begin{cases} \partial_t H(t, \xi) + \dfrac{1}{\varepsilon^2} \partial_\xi H(t, \xi) = \varepsilon^2 G(t, \xi) + F_{[H]}(t, \xi), \quad t > 0, \ \xi \in \mathbb{T}, \\ H(0, \xi) = \varepsilon^2 \left[\Theta\left(0, \xi, v_0\right) - \Theta\left(0, \xi, \underline{w}(0)\right)\right], \quad \xi \in \mathbb{T}. \end{cases} \tag{3.13}$$

One can observe that

$$\|H(0, \cdot)\|_{H^1(\mathbb{T}) \times H^{m_0+4}(\mathbb{R}^d)} \lesssim \varepsilon^4 \quad \text{and} \quad H(0, 0) = h(0),$$

which by the uniqueness of the solution leads to

$$H(t, t/\varepsilon^2) = h(t), \quad t \geq 0. \tag{3.14}$$

Take Fourier transform of (3.13) on the ξ,

$$\partial_t \widehat{H}_l(t) + \dfrac{il}{\varepsilon^2} \widehat{H}_l(t) = \varepsilon^2 \widehat{G}_l(t) + \widehat{(F_{[H]})}_l(t), \quad t > 0, \ l \in \mathbb{N}.$$

By Duhamel's formula, we get

$$\widehat{H}_l(t) = e^{-ilt/\varepsilon^2} \widehat{H}_l(0) + \int_0^t e^{-il(t-s)/\varepsilon^2} \left[\varepsilon^2 \widehat{G}_l(s) + \widehat{(F_{[H]})}_l(s)\right] ds. \tag{3.15}$$

We carry out an integration-by-parts for $l \neq 0$,

$$\int_0^t e^{-il(t-s)/\varepsilon^2} \varepsilon^2 \widehat{G}_l(s) ds = -\dfrac{\varepsilon^4 i}{l} \left(\widehat{G}_l(t) - e^{-ilt/\varepsilon^2} \widehat{G}_l(0)\right)$$

$$+ \dfrac{\varepsilon^4 i}{l} \int_0^t e^{-il(t-s)/\varepsilon^2} \widehat{G}_l'(s) ds,$$

with noting meanwhile

$$\widehat{G}_0(t) = \Pi G(t, \cdot) = 0, \quad t \geq 0.$$

From (3.10) and the regularity of the limit model (3.9), we can find

$$\|\partial_t \Theta(t,\cdot,\underline{w}(t))\|_{H^1(\mathbb{T}) \times H^{m_0+2}(\mathbb{R}^d)} \lesssim 1, \quad \|\partial_t^2 \Theta(t,\cdot,\underline{w}(t))\|_{H^1(\mathbb{T}) \times H^{m_0}(\mathbb{R}^d)} \lesssim 1,$$

and therefore we can further have

$$\|G(t,\cdot)\|_{H^1(\mathbb{T}) \times H^{m_0+2}(\mathbb{R}^d)} \lesssim 1, \quad \|\partial_t G(t,\cdot)\|_{H^1(\mathbb{T}) \times H^{m_0}(\mathbb{R}^d)} \lesssim 1.$$

Then by squaring (3.15) and using Hölder's inequality and Parserval's identity, we get

$$\|H(t,\cdot)\|_{H^1(\mathbb{T}) \times H^{m_0}(\mathbb{R}^d)} \lesssim \varepsilon^4 + \int_0^t \|F_{[H]}(s,\cdot)\|_{H^1(\mathbb{T}) \times H^{m_0}(\mathbb{R}^d)} ds.$$

Thanks to the fact:

$$F_{[H]}(t,\xi) = O(H(t,\xi)),$$

by a bootstrap argument, one can get

$$\|H(t,\cdot)\|_{H^1(\mathbb{T}) \times H^{m_0}(\mathbb{R}^d)} \lesssim \varepsilon^4, \quad 0 \leq t \leq T,$$

for some $T > 0$ independent of ε. Finally using (3.14) and the Sobolev imbedding,

$$\|h(t)\|_{H^1(\mathbb{R}^d)} \lesssim \|H(t,\cdot)\|_{L^\infty(\mathbb{T}) \times H^1(\mathbb{R}^d)} \lesssim \varepsilon^4, \quad 0 \leq t \leq T.$$

$$\square$$

Again by defining

$$u_{CE}(\mathbf{x},t) := \frac{1}{2} \left[e^{it/\varepsilon^2 \sqrt{1-\varepsilon^2 \Delta}} \left(\underline{w}(\mathbf{x},t) + \varepsilon^2 \Theta(t, t/\varepsilon^2, \underline{w}(\mathbf{x},t)) \right) + c.c. \right], \qquad (3.16)$$

we get the next order Chapman-Enskog expansion for KG (1.1) as

$$u(\mathbf{x},t) = u_{CE}(\mathbf{x},t) + o(\varepsilon^2), \quad \varepsilon \to 0.$$

Corollary 3.5. *Define* $R(\mathbf{x},t) = u(\mathbf{x},t) - u_{CE}(\mathbf{x},t)$. *Under the assumption that* $\phi_1, \phi_2 \in H^{m_0+4}(\mathbb{R}^d)$, $m_0 > d/2$, *we have*

$$\|R(\cdot,t)\|_{H^{m_0}} \lesssim \varepsilon^4, \quad 0 \leq t \leq T, \qquad (3.17)$$

for some T independent of ε and $0 < T < T^*$.

We see that similarly to the high order multiscale frequency expansion, the high order Chapman-Enskog expansion (3.16) is also in a rather compact form. That is to say, the expansion (3.16) only involves a limit equation, i.e. (3.9) to solve. However, the limit equation (3.9) is much more complicated than (3.5). Note that again (3.9) can be solved by a finite time difference integrator.

3.4. **Dynamics and comparisons.** We consider again the one dimensional KG to study and compare the high order versions of the three expansions.

Example 3.6 (Comparison in accuracy)**.** Firstly, we compare the remainders of the three expansions at a fixed time. The remainders R_{MFo} R_{MFe} and R_{CE} measured in a discrete H^1-norm at $T = 0.5$ and $T = 1$ with initial values (2.18) are shown in Table 3. The results show that the higher order MFe expansion is the most accurate approximation to the KG.

TABLE 3. Remainders (in H^1-norm) of the next order modulated Fourier (MFo) expansion, the multiscale frequency (MFe) expansion and the Chapman-Enskog (CE) expansion.

$t = 0.5$	$\varepsilon = 0.1$	$\varepsilon/2$	$\varepsilon/2^2$	$\varepsilon/2^3$
MFo	2.30E-2	2.30E-3	1.82E-4	1.20E-5
MFe	4.99E-6	1.61E-7	1.06E-8	6.69E-10
CE	3.64E-5	1.87E-6	1.20E-7	7.29E-9
$t = 1$	$\varepsilon = 0.1$	$\varepsilon/2$	$\varepsilon/2^2$	$\varepsilon/2^3$
MFo	5.68E-2	7.60E-3	6.84E-4	4.61E-5
MFe	3.03E-6	2.42E-7	1.56E-8	1.23E-9
CE	2.20E-5	1.58E-6	1.03E-7	6.48E-9

Example 3.7 (Dynamics of remainder). Next, we study the long-time behavior of the expansions under smooth initial data. The dynamics of the remainder terms R_{MFo}, R_{MFe} and R_{CE} of three expansions in H^1 divided by ε^4 in the whole space case (2.18) and torus (2.19) are plotted in Figure 8. From the results, we can see: 1) In the whole space case, the remainder of MFo increases with time rapidly, but in the torus case it increases linearly. 2) In the whole space case, the remainder of MFe has an increasing drift, while CE has remainder uniformly bounded in time. 3) In the torus case, the remainders of both MFe and CE start to increase after some time, but MFe has less increment.

Example 3.8 (Energy conservation). The relative energy error $|\mathcal{H}(t)-H(0)|/|H(0)|$ by using the next order expansions under case (2.18) or (2.19) is plotted in Figure 9. The results show: 1) The energy by the expansions converges relatively with rate $O(\varepsilon^4)$ to the exact energy. 2) CE has uniformly bounded energy error with respect to time. 3) MFe in the whole space case has a drift in the error similarly as the behavior of the remainder. In the torus case, the error of MFe is bouncing.

Example 3.9 (Comparison in regularity). At last but not least, we test the behavior of the remainders of the high order expansions under the initial data of lower regularity (2.20) on the torus. We plot in Figure 10 the dynamics of the remainders $\|R_{MFo}\|_{H^1}/\varepsilon^4$ under H^7-data or H^8-data, $\|R_{MFe}\|_{H^1}/\varepsilon^4$ and $\|R_{CE}\|_{H^1}/\varepsilon^4$ under H^3-data or H^4-data. Based on the numerical results, we observe that $\|R_{MFo}\|_{H^1} = O(\varepsilon^4)$ under H^8-data and $\|R_{MFe}\|_{H^1}$, $\|R_{CE}\|_{H^1} = O(\varepsilon^4)$ under H^4-data. All the three expansions seem to hold the fourth order convergence rate in ε with less required regularity than the analytical results in Lemmas 3.1-3.5. Certainly more dedicated and deep analysis is needed to seek for the sharp regularity requirement.

4. CONCLUSION

We studied and compared three kinds of popular asymptotic expansions applied to the nonlinear Klein-Gordon equation in the nonrelativistic limit regime. The expansions include the modulated Fourier expansion, multiscale expansion by frequency and the Chapman-Enskog expansion up to the leading and higher order
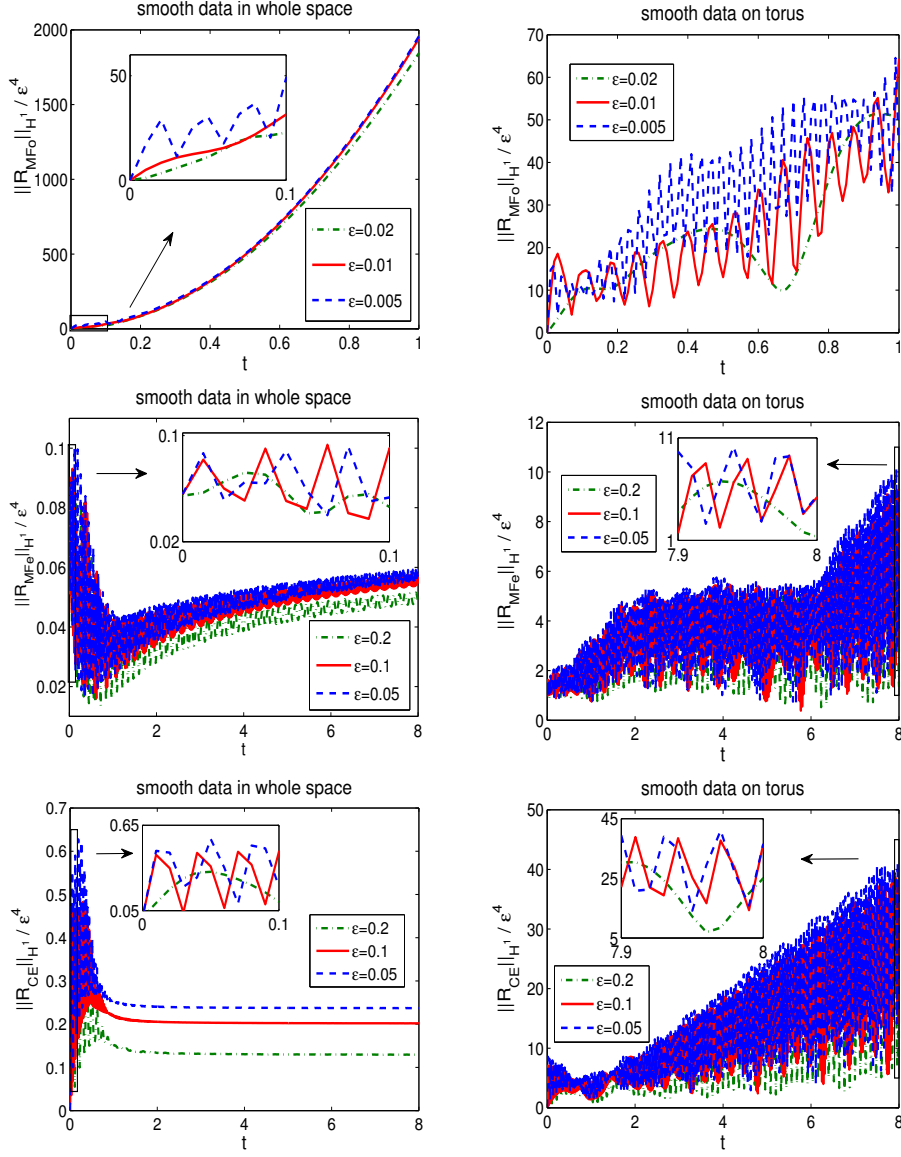
FIGURE 8. Behavior of the remainder terms $\|R_{MFo}\|_{H^1}/\varepsilon^4$, $\|R_{MFe}\|_{H^1}/\varepsilon^4$ and $\|R_{CE}\|_{H^1}/\varepsilon^4$ with respect to time under two cases: initial smooth localized wave (2.18) in $\mathbb{R}$ (left) and smooth planewave (2.19) on torus $\mathbb{T}$ (right).

term. The comparisons of the expansions were made on the accuracy, the regularity and the dynamics. We commented on the advantages and disadvantages of each expansion.
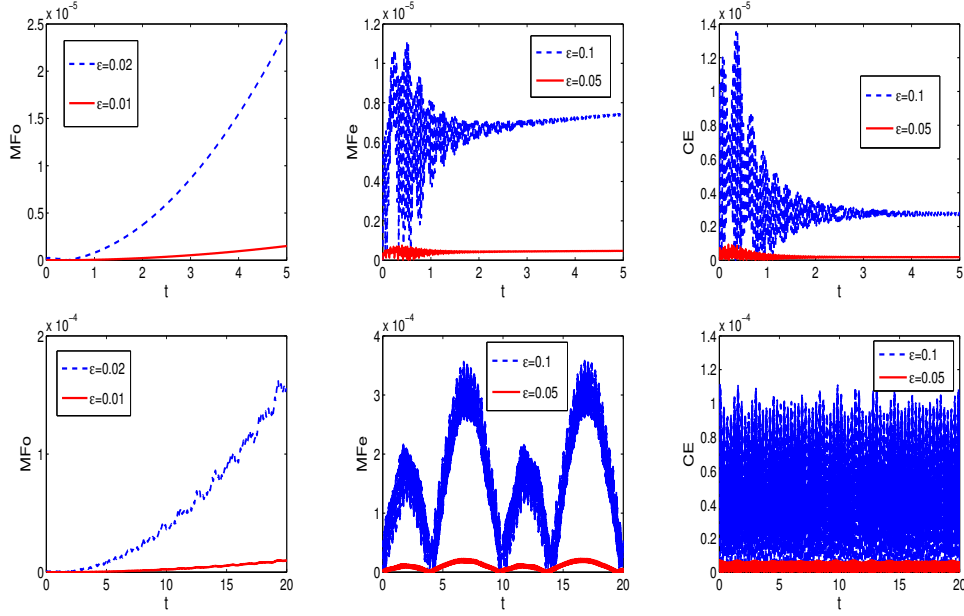
FIGURE 9. Energy error $|\mathcal{H}(t) - H(0)|/|H(0)|$ of the three expansions to the next order under whole space case (up) and torus case (down).

Acknowledgements

References

[1] D.D. BAĬNOV AND E. MINCHEV, Nonexistence of global solutions of the initial-boundary value problem for the nonlinear Klein-Gordon equation, J. Math. Phys. 36 (1995) pp. 756-762.

[2] W. BAO, Y. CAI, Uniform error estimates of finite difference methods for the nonlinear Schrödinger equation with wave operator, SIAM J. Numer. Anal. 50 (2012) pp. 492-521.

[3] W. BAO, Y. CAI, Uniform and optimal error estimates of an exponential wave integrator sine pseudospectral method for the nonlinear Schrödinger equation with wave operator, SIAM J. Numer. Anal. 52 (2014) pp. 1103-1127.

[4] W. BAO, Y. CAI, X. ZHAO, A uniformly accurate multiscale time integrator pseudospectral method for the Klein-Gordon equation in the nonrelativistic limit regime, SIAM J. Numer. Anal. 52 (2014) pp. 2488-2511.

[5] W. BAO, X. DONG, Analysis and comparison of numerical methods for the Klein-Gordon equation in the nonrelativistic limit regime, Numer. Math. 120 (2012) pp. 189-229.

[6] W. BAO, X. DONG, X. ZHAO, Uniformly accurate multiscale time integrators for highly oscillatory second order differential equations, J. Math. Study 47 (2014) pp. 111-150.

[7] S. BAUMSTARK, E. FAOU, K. SCHRATZ, Uniformly accurate exponential-type integrators for Klein-Gordon equations with asymptotic convergence to the classical NLS splitting, to appear in Math. Comp. doi:10.1090/mcom/3263.
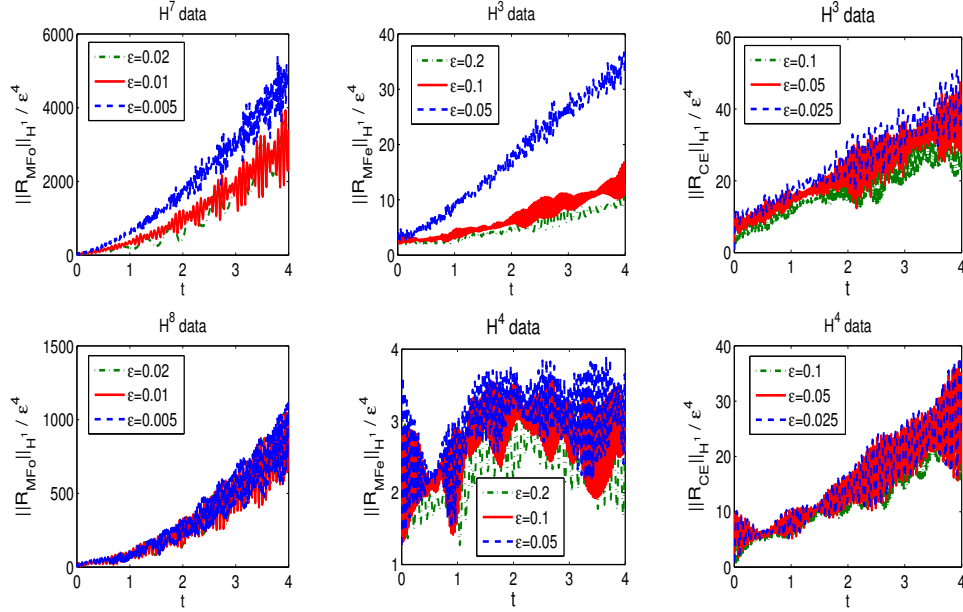
FIGURE 10. Behavior of the remainders under lower regularity initial data (2.20).

[8] W. BAO, X. ZHAO, A uniformly accurate (UA) multiscale time integrator Fourier pseoduspectral method for the Klein-Gordon-Schrödinger equations in the nonrelativistic limit regime, Numer. Math. 135 (2017) pp. 833-873.

[9] W. BAO, X. ZHAO, A uniformly accurate multiscale time integrator pseudospectral method for the Klein-Gordon-Zakharov system in the high-plasma-frequency limit regime, J. Comput. Phys. 327 (2016) pp. 270-293.

[10] W. BAO, X. ZHAO, A uniform second-order in time multiscale time integrator for the nonlinear Klein-Gordon equation in the nonrelativistic limit regime, preprint (2017).

[11] S. CHAPMAN, T.G. COWLING, D. BURNETT, The mathematical theory of non-uniform gases: an account of the kinetic theory of viscosity, thermal conduction, and diffusion in gases. Cambridge University Press, 1970.

[12] PH. CHARTIER, N. CROUSEILLES, M. LEMOU, F. MÉHATS, Uniformly accurate numerical schemes for highly oscillatory Klein-Gordon and nonlinear Schrödinger equations, Numer. Math. 129 (2015) pp. 211-250.

[13] P. CHARTIER, M. LEMOU, F. MÉHATS AND G. VILMART, Uniformly accurate averaging methods, preprint (2017).

[14] N. CROUSEILLES, M. LEMOU, F. MÉHATS, Asymptotic Preserving schemes for highly oscillatory Vlasov-Poisson equations, J. Comput. Phys. 248 (2013) pp. 287-308.

[15] D. COHEN, E. HAIRER, CH. LUBICH, Modulated Fourier expansions of highly oscillatory differential equations, Found. Comput. Math. 3 (2003) pp. 327-345.

[16] A.S. DAVYDOV, Quantum Mechanics, 2nd edn. Pergamon, Oxford, 1976.

[17] X. DONG, Z. XU, X. ZHAO, On time-splitting pseudospectral discretization for nonlinear Klein-Gordon equation in nonrelativistic limit regime, Commun. Comput. Phys. 16 (2014) pp. 440-66.

[18] E. FAOU, L. GAUCKLER AND CH. LUBICH, Sobolev stability of plane wave solutions to the cubic nonlinear Schrödinger equation on a torus, Comm. Partial Differential Equations 38 (2013), pp. 1123-1140.

[19] E. FAOU, K. SCHRATZ, Asympotic preserving schemes for the Klein- Gordon equation in the non-relativistic limit regime, Numer. Math. 126 (2014) pp. 441-469.

[20] K. Huang, C. Xiong and X. Zhao, Scalar-field theory of dark matter, Inter. J. Modern Physics A 29 (2014) article 1450074.

[21] E. Hairer, Ch. Lubich, G. Wanner, Geometric Numerical Integration: Structure-Preserving Algorithms for Ordinary Differential Equations, Springer, Berlin, 2006.

[22] M. Hochbruck, A. Ostermann, Exponential integrators, Acta Numer. 19 (2010) pp. 209-286.

[23] C. Lubich, On splitting methods for Schrödinger-Poisson and cubic nonlinear Schrödinger equations. Math. Comp. 77 (2008) pp. 2141-2153.

[24] S. Machihara, K. Nakanishi, T. Ozawa, Nonrelativistic limit in the energy space for nonlinear Klein-Gordon equations, Math. Ann. 322 (2002) pp. 603-621.

[25] N. Masmoudi, K. Nakanishi, From nonlinear Klein-Gordon equation to a system of coupled nonlinear Schrödinger equations, Math. Ann. 324 (2002) pp. 359-389.

[26] B. Najman, The nonrelativistic limit of the nonlinear Klein-Gordon equation, Nonlinear Anal. 15 (1990) pp. 217-228.

[27] A. Ostermannm, K. Schratz Low regularity exponential-type integrators for semilinear Schrödinger equations, Found. Comput. Math. (2017) doi:10.1007/s10208-017-9352-1.

[28] S. Pascali, Dynamics of the nonlinear Klein-Gordon equation in the nonrelativistic limit, preprint arxiv:1703.01609.

[29] C. Xiong, M.R.R. Good, Y. Guo, X. Liu and K. Huang, Relativistic superfluidity and vorticity from the nonlinear Klein-Gordon equation, Phys. Rev. D 90 (2014) article 125019.

[30] X. Zhao, A combination of multiscale time integrator and two-scale formulation for the nonlinear Schroinger equation with wave operator, J. Comput. Appl. Math. 326 (2017) pp. 320-336.

K. Schratz: Fakultät für Mathematik, Karlsruhe Institute of Technology, Germany
    E-mail address: katharina.schratz@kit.edu

X. Zhao: Fakultät für Mathematik, Karlsruhe Institute of Technology, Germany
    E-mail address: zhxfnus@gmail.com